

1	2	3	4	5	6	7	8	9	10	11	12	13	14	15	16	17	18	19	20	21	22	23	24	25	26	27	28	29	30	31	32	33	34	35	36	37	38	39	40	41	42	43	44	45	46	47	48	49	50	51	52	53	54	55	56	57	58	59	60	61	62	63	64	65	66	67	68	69	70	71	72	73	74	75	76	77	78	79	80	81	82	83	84	85	86	87	88	89	90	91	92	93	94	95	96	97	98	99	100	101	102	103	104	105	106	107	108	109	110	111	112	113	114	115	116	117	118	119	120	121	122	123	124	125	126	127	128	129	130	131	132	133	134	135	136	137	138	139	140	141	142	143	144	145	146	147	148	149	150	151	152	153	154	155	156	157	158	159	160	161	162	163	164	165	166	167	168	169	170	171	172	173	174	175	176	177	178	179	180	181	182	183	184	185	186	187	188	189	190	191	192	193	194	195	196	197	198	199	200	201	202	203	204	205	206	207	208	209	210	211	212	213	214	215	216	217	218	219	220	221	222	223	224	225	226	227	228	229	230	231	232	233	234	235	236	237	238	239	240	241	242	243	244	245	246	247	248	249	250	251	252	253	254	255	256	257	258	259	260	261	262	263	264	265	266	267	268	269	270	271	272	273	274	275	276	277	278	279	280	281	282	283	284	285	286	287	288	289	290	291	292	293	294	295	296	297	298	299	300	301	302	303	304	305	306	307	308	309	310	311	312	313	314	315	316	317	318	319	320	321	322	323	324	325	326	327	328	329	330	331	332	333	334	335	336	337	338	339	340	341	342	343	344	345	346	347	348	349	350	351	352	353	354	355	356	357	358	359	360	361	362	363	364	365	366	367	368	369	370	371	372	373	374	375	376	377	378	379	380	381	382	383	384	385	386	387	388	389	390	391	392	393	394	395	396	397	398	399	400	401	402	403	404	405	406	407	408	409	410	411	412	413	414	415	416	417	418	419	420	421	422	423	424	425	426	427	428	429	430	431	432	433	434	435	436	437	438	439	440	441	442	443	444	445	446	447	448	449	450	451	452	453	454	455	456	457	458	459	460	461	462	463	464	465	466	467	468	469	470	471	472	473	474	475	476	477	478	479	480	481	482	483	484	485	486	487	488	489	490	491	492	493	494	495	496	497	498	499	500	501	502	503	504	505	506	507	508	509	510	511	512	513	514	515	516	517	518	519	520	521	522	523	524	5
---	---	---	---	---	---	---	---	---	----	----	----	----	----	----	----	----	----	----	----	----	----	----	----	----	----	----	----	----	----	----	----	----	----	----	----	----	----	----	----	----	----	----	----	----	----	----	----	----	----	----	----	----	----	----	----	----	----	----	----	----	----	----	----	----	----	----	----	----	----	----	----	----	----	----	----	----	----	----	----	----	----	----	----	----	----	----	----	----	----	----	----	----	----	----	----	----	----	----	-----	-----	-----	-----	-----	-----	-----	-----	-----	-----	-----	-----	-----	-----	-----	-----	-----	-----	-----	-----	-----	-----	-----	-----	-----	-----	-----	-----	-----	-----	-----	-----	-----	-----	-----	-----	-----	-----	-----	-----	-----	-----	-----	-----	-----	-----	-----	-----	-----	-----	-----	-----	-----	-----	-----	-----	-----	-----	-----	-----	-----	-----	-----	-----	-----	-----	-----	-----	-----	-----	-----	-----	-----	-----	-----	-----	-----	-----	-----	-----	-----	-----	-----	-----	-----	-----	-----	-----	-----	-----	-----	-----	-----	-----	-----	-----	-----	-----	-----	-----	-----	-----	-----	-----	-----	-----	-----	-----	-----	-----	-----	-----	-----	-----	-----	-----	-----	-----	-----	-----	-----	-----	-----	-----	-----	-----	-----	-----	-----	-----	-----	-----	-----	-----	-----	-----	-----	-----	-----	-----	-----	-----	-----	-----	-----	-----	-----	-----	-----	-----	-----	-----	-----	-----	-----	-----	-----	-----	-----	-----	-----	-----	-----	-----	-----	-----	-----	-----	-----	-----	-----	-----	-----	-----	-----	-----	-----	-----	-----	-----	-----	-----	-----	-----	-----	-----	-----	-----	-----	-----	-----	-----	-----	-----	-----	-----	-----	-----	-----	-----	-----	-----	-----	-----	-----	-----	-----	-----	-----	-----	-----	-----	-----	-----	-----	-----	-----	-----	-----	-----	-----	-----	-----	-----	-----	-----	-----	-----	-----	-----	-----	-----	-----	-----	-----	-----	-----	-----	-----	-----	-----	-----	-----	-----	-----	-----	-----	-----	-----	-----	-----	-----	-----	-----	-----	-----	-----	-----	-----	-----	-----	-----	-----	-----	-----	-----	-----	-----	-----	-----	-----	-----	-----	-----	-----	-----	-----	-----	-----	-----	-----	-----	-----	-----	-----	-----	-----	-----	-----	-----	-----	-----	-----	-----	-----	-----	-----	-----	-----	-----	-----	-----	-----	-----	-----	-----	-----	-----	-----	-----	-----	-----	-----	-----	-----	-----	-----	-----	-----	-----	-----	-----	-----	-----	-----	-----	-----	-----	-----	-----	-----	-----	-----	-----	-----	-----	-----	-----	-----	-----	-----	-----	-----	-----	-----	-----	-----	-----	-----	-----	-----	-----	-----	-----	-----	-----	-----	-----	-----	-----	-----	-----	-----	-----	-----	-----	-----	-----	-----	-----	-----	-----	-----	-----	-----	-----	-----	-----	-----	-----	-----	-----	-----	-----	-----	-----	-----	-----	-----	-----	-----	-----	-----	-----	-----	-----	-----	-----	-----	-----	-----	-----	-----	-----	-----	-----	-----	-----	-----	-----	-----	-----	-----	-----	-----	-----	-----	-----	-----	-----	-----	-----	-----	-----	-----	---

COVER SHEET FOR TECHNICAL MEMORANDUM

TITLE- Influence of Vehicle Dynamics on the
Artificial Gravity Experiment on the
Second Saturn Workshop

TM- 70-1022-5

FILING CASE NO(S)- 620

DATE- April 17, 1970

AUTHOR(S)- L. E. Voelker

FILING SUBJECT(S) Apollo Applications Program
(ASSIGNED BY AUTHOR(S))- Artificial Gravity
Rotational Dynamics

ABSTRACT

A proposed artificial gravity experiment for the second AAP Workshop would be performed by spinning the vehicle and using the resulting centrifugal forces to simulate gravitational forces. If, as in the first Workshop, power is obtained from solar arrays, then the vehicle must be rotated about an axis normal to the arrays, and this axis must be aligned with the solar vector.

The Euler equations of motion governing rigid body rotation are used to study the dynamic behavior of a Workshop of the same configuration as the first Workshop. In the absence of external torques, the results show that the solar arrays cannot be kept pointed at the sun and that the dynamic behavior is generally unacceptable. The ATM control moment gyros are clearly inadequate for control of this configuration. Various other configurations are studied and evaluated. Configurations that show promise of good dynamic behavior include ballast on deployable booms 40 to 100 feet in length.

The primary conclusion is that some modification of the Workshop configuration is required to provide acceptable rotational dynamics for the artificial gravity mode.

DISTRIBUTIONCOMPLETE MEMORANDUM TO

CORRESPONDENCE FILES:

OFFICIAL FILE COPY

plus one white copy for each
additional case referenced

TECHNICAL LIBRARY (4)

NASA Headquarters

W. O. Armstrong/MTX
H. Cohen/MLR
P. E. Culbertson/MT
J. H. Disher/MLD
W. B. Evans/MLO
L. K. Fero/MLV
J. P. Field, Jr./MLP
W. D. Green, Jr./MLA
W. H. Hamby/MLO
J. L. Hammersmith/MTP
T. E. Hanes/MLA
B. Maggin/PT
M. Savage/MLT
W. C. Schneider/ML

LaRC

P. R. Kurzhals/AMPD

MSC

O. K. Garriott/CB
F. C. Littleton/KM
C. F. Lively/EG23
A. J. Louviere/ET
O. G. Smith/KF

MSFC

W. B. Chubb/S&E-ASTR-SGD
B. J. Clingman/PM-AA
C. R. Ellsworth/PD-AP-S
G. A. Keller/PD-SS-T
E. F. Noel/S&E-ASTR-SI

COVER SHEET ONLY TOCOMPLETE MEMORANDUM TO, continuedMartin-Marietta/Denver

G. Rodney

McDonnell-Douglas/East

M. Czarnik

McDonnell-Douglas/West

R. S. Buchanan
H. Curtis
R. J. Thiele

North American Rockwell

R. Westrup/SL-51

Bellcomm, Inc.

A. P. Boysen
D. R. Hagner
B. T. Howard
C. E. Johnson
R. K. McFarland
R. E. McGaughy
J. Z. Menard
P. F. Sennewald
R. V. Sperry
J. W. Timko
M. P. Wilson
Department 1022
Divisions 101, 102 Supervision
Department 1024 File
Central Files

ABSTRACT ONLY:

I. M. Ross
R. L. Wagner

BELLCOMM. INC.

955 L'ENFANT PLAZA NORTH, S.W.

WASHINGTON, D. C. 20024

SUBJECT: Influence of Vehicle Dynamics on the
Artificial Gravity Experiment on the
Second Saturn Workshop - Case 620

DATE: April 17, 1970

FROM: L. E. Voelker

TM-70-1022-5

TECHNICAL MEMORANDUM

1.0 INTRODUCTION

An artificial gravity experiment has been proposed for the second Saturn Workshop; it would be conducted during portions of one or more of the CSM missions. Artificial gravity would be obtained by spinning the vehicle about its center of mass. If the source of power during the artificial gravity experiment is to be solar arrays, and if these are fixed perpendicular to the vehicle z-axis as in the first Workshop, then this axis should be the axis of rotation and should be oriented along the solar vector. This paper considers the dynamical problems of spinning up and rotating various Workshop configurations about the sun-oriented vehicle z-axis.

The centrifugal force due to the rotation of the Cluster will induce radial loads on some components which may necessitate modification of various load bearing structures. Deployed components, such as the Workshop solar arrays, the Apollo Telescope Mount, and its solar arrays are particularly vulnerable. Examples of component loads at the end of the spin-up phase are presented. No conclusions on structural adequacy are drawn, however, as the actual loads will depend on angular acceleration and velocity limits which are not yet determined. To determine these limits, more investigation is required, and in the final section a list of specific items that require further study is given.

1.1 Envelope of Parameters for Experiment

The purpose of the artificial gravity experiment is to investigate the alleviating effects of an artificial gravity environment upon problems which might occur in a long-term zero-gravity environment. These problems are of two types: physiological ones, including the effects on the cardiovascular system, muscles, skeleton, and the reflexes; and habitability problems such as floating debris, mobility, manipulation of

objects and the containment of fluids. However, the rotating vehicle produces its own set of peculiar difficulties for the astronauts. These include physiological effects such as canal sickness caused by over-stimulation of the vestibular organs [1]*, a gradient between the levels of induced gravity at the head and feet, and habitability problems such as the unusual kinematics of falling or thrown objects [2]. An uncontrolled rotating vehicle, when disturbed, will wobble (a curvilinear oscillatory motion of the spin axis), contributing to all of the above effects [3]. These and other physiological and habitability effects can be used to formulate limits of acceptability on angular velocity, artificial gravity level, and spin radius. The envelope of acceptability proposed by the Manned Spacecraft Center consists of the following limits:

	<u>Minimum</u>	<u>Maximum</u>	
Spin Radius	30	150	feet
Angular Velocity	2	10	rpm
Artificial Gravity Level	.2	.8	G

This envelope and those proposed in References [1] and [3] are outlined in Figure 1.

2.0 ANALYSIS

2.1 General Equations of Motion

The equations for angular motion of a body with respect to an inertial reference frame may be written as

$$\underline{\dot{M}} = \underline{\dot{H}} \quad (1)$$

where

\underline{M} = the external applied moment vector

\underline{H} = the total angular momentum vector of the body

$(\dot{})$ = differentiation with respect to time.

If the body is a vehicle containing rotors or gyroscopes, equation (1) can be written in inertial coordinates as

$$\underline{\dot{M}} = (\underline{\dot{I}}\underline{\omega}) + \underline{\dot{H}}_g \quad (2)$$

*Numbers in brackets refer to references listed at the end of this report.

where

I = the inertia tensor of the vehicle

$\underline{\omega}$ = the angular velocity vector of the vehicle

\underline{H}_g = the angular momentum vector of the vehicle's gyros.

Two representative terms of the symmetric inertia tensor are given by:

$$I_{xx} = \int_V \rho (y^2 + z^2) dV \quad (3)$$

$$I_{yz} = - \int_V \rho yz dV \quad (4)$$

where $\rho(x,y,z)$ is the mass distribution of the vehicle. The remaining terms are found through permutations of x, y , and z .

When written in terms of body-fixed vehicle coordinates, equation (2) becomes

$$\underline{M} = I \dot{\underline{\omega}} + \underline{\omega} \times I \underline{\omega} + \dot{\underline{H}}_g + \underline{\omega} \times \underline{H}_g \quad (5)$$

2.2 Torque-Free Motion of a Rigid Vehicle

The particular case of "torque-free" motion (the external moment is zero) of a vehicle without gyros is governed by the following equation:

$$0 = I \dot{\underline{\omega}} + \underline{\omega} \times I \underline{\omega} \quad (6)$$

If the expressions for the kinetic energy T and the magnitude of the angular momentum vector H are recognized as

$$T = \frac{1}{2} (\underline{\omega} \cdot \underline{I} \underline{\omega}) \quad (7)$$

$$H = (\underline{I} \underline{\omega} \cdot \underline{I} \underline{\omega})^{1/2} \quad (8)$$

both of which remain constant for torque-free motion, then equation (6) can be solved analytically (see the Appendix). The analytic solutions are of two distinct types. The first type takes the form of a constant rotation about one of the principal inertial axes. In the second type of solution, the components of angular velocity are periodic functions, specifically, the Jacobian elliptic functions, as described in the Appendix. In either case, if there is any internal damping in the vehicle, the angular velocity vector will ultimately coincide with the axis of maximum principal inertia.

2.3 Torque-free Motion of a Vehicle with Gyroscopes

The governing equation in body-fixed coordinates for torque-free ($\underline{M} \equiv 0$) motion of a vehicle with gyroscopes is

$$\underline{I} \dot{\underline{\omega}} + \underline{\omega} \times \underline{I} \underline{\omega} + \underline{\dot{H}}_g + \underline{\omega} \times \underline{H}_g = 0. \quad (9)$$

We will specify that the vehicle is rotating about its geometric z-axis, as desired, with a constant angular velocity ω_z . thus, equation (9) becomes

$$\underline{\omega} \times \underline{I} \underline{\omega} + \underline{\dot{H}}_g + \underline{\omega} \times \underline{H}_g = 0. \quad (10)$$

For $\underline{\omega} = (0, 0, \omega_z)$, equation (10) can be expanded into the following scalar equations

$$\omega_z^2 I_{yz} - \dot{H}_{gx} + \omega_z H_{gy} = 0 \quad (11a)$$

$$\omega_z^2 I_{xz} + \dot{H}_{gy} + \omega_z H_{gx} = 0 \quad (11b)$$

$$\dot{H}_{gz} = 0 \quad (11c)$$

where $\underline{H}_g = (H_{gx}, H_{gy}, H_{gz})$.

The gyroscopes can be initialized such that their momentum components along the spacecraft x and y axes are constant, and there is no component along the z-axis. With such initial conditions, the solutions to (11) are

$$H_{gx} = -\omega_z I_{xz} \quad (12a)$$

$$H_{gy} = -\omega_z I_{yz} \quad (12b)$$

$$H_{gz} = 0.$$

The smallest possible magnitude of gyroscope angular momentum that will maintain steady rotation about the vehicle z-axis is, therefore,

$$|\underline{H}_g|_{\text{MIN}} = \omega_z \left(I_{xz}^2 + I_{yz}^2 \right)^{1/2}. \quad (13)$$

2.4 Euler Angles

The Euler angles are used to describe the position of a body undergoing arbitrary rotation about its center of gravity (CG). If the body-fixed coordinate axes xyz are initially coincident with an inertial reference frame denoted by coordinate axes XYZ, then, by specifying three successive rotations in a particular sequence, any orientation of the body with respect to the XYZ axes can be described.

In Figure 2, a positive rotation ψ about the Z-axis generates $x'y'Z$; a rotation θ about x' produces $x'y''z$; and finally, a rotation ϕ about z results in the xyz body-fixed coordinate axes.

It is apparent that any possible orientation of the axes xyz can be attained by performing the proper rotations in the specified order. It is noted that the Euler angle θ is the angle between the inertial Z -axis and the body-fixed z -axis.

By inspecting the projections of the Euler angle rates on the xyz axes, the components of the angular velocity vector $\underline{\omega}$, in body-fixed coordinate axes, can be written

$$\omega_x = \dot{\psi} s\theta s\phi + \dot{\theta} c\phi \quad (14a)$$

$$\omega_y = \dot{\psi} s\theta c\phi - \dot{\theta} s\phi \quad (14b)$$

$$\omega_z = \dot{\phi} + \dot{\psi} c\theta \quad (14c)$$

where we have defined $s\theta \equiv \sin\theta$, $s\phi \equiv \sin\phi$, $c\theta \equiv \cos\theta$, and $c\phi \equiv \cos\phi$.

Equations (14) possess the following inverse relations

$$\dot{\theta} = \omega_x c\phi - \omega_y s\phi \quad (15a)$$

$$\dot{\psi} = (\omega_x s\phi + \omega_y c\phi)/s\theta \quad (15b)$$

$$\dot{\phi} = \omega_z - \dot{\psi} c\theta \quad (15c)$$

In order to write a vector given in body-fixed coordinate axes in terms of the inertial coordinate axes, the transformation matrix is required. Referring back to the definitions of θ , ψ , ϕ and writing out the rotations in matrix form, we have

$$(x', y', z) = [\psi] (X, Y, Z) \quad (16a)$$

$$(x', y'', z) = [\theta] (x', y', z) \quad (16b)$$

$$(x, y, z) = [\phi] (x', y'', z) \quad (16c)$$

where, for example,

$$[\psi] = \begin{bmatrix} c\psi & s\psi & 0 \\ -s\psi & c\psi & 0 \\ 0 & 0 & 1 \end{bmatrix} \quad (17)$$

and $c\psi \equiv \cos\psi$, $s\psi \equiv \sin\psi$.

Thus, the transformation relation is

$$\underline{r} = [A] \underline{R} \quad (18)$$

where

$$[A] = [\phi] [\theta] [\psi] . \quad (19)$$

\underline{R} is a vector in inertial (XYZ) coordinates and \underline{r} is the same vector in body (xyz) coordinates.

In the same way,

$$\underline{R} = [a] \underline{r} \quad (20)$$

and the transformation matrix is, in full,

$$[a] = \begin{bmatrix} c\psi c\phi - s\psi c\theta s\phi & -s\psi c\theta c\phi - c\psi s\phi & s\psi s\theta \\ s\psi c\phi + c\psi c\theta s\phi & c\psi c\theta c\phi - s\psi s\phi & -c\psi s\theta \\ s\theta s\phi & s\theta c\phi & c\theta \end{bmatrix} \quad (21)$$

which transforms from body-fixed vehicle coordinates to inertial coordinates. The matrix $[a]$ is the inverse of $[A]$, and as any matrix of direction cosines is orthogonal, it is also the transpose of $[A]$.

2.5 Method of Solution

Of primary interest in this study is the dynamic behavior of the vehicle without gyroscopes, governed by the equation

$$\underline{\dot{M}} = \underline{I}\underline{\dot{\omega}} + \underline{\omega} \times \underline{I}\underline{\omega} \quad (22)$$

from equation (5) and which can be rewritten in the form

$$\underline{\dot{\omega}} = \underline{I}^{-1} (\underline{M} - \underline{\omega} \times \underline{I}\underline{\omega}) \quad (23)$$

where \underline{I}^{-1} is the inverse of the inertia matrix \underline{I} .

For a given set of initial conditions for $\underline{\omega}$, θ , ψ and ϕ , equations (15) and (23) give the corresponding initial values for $\underline{\dot{\omega}}$, $\dot{\theta}$, $\dot{\psi}$, $\dot{\phi}$. A computer program employing a modified Runge-Kutta numerical procedure for solving a system of first order differential equations is then called upon to predict values at stated increments of time. The Euler angle θ , which is the angle between the inertial Z-axis and the body-fixed z-axis, is defined non-negative, so if the numerical computation predicts a negative value for θ , control is returned to the previous time step, the step-size is reduced, and new values are calculated until the predicted values of θ remain positive.

The program was checked against the known analytical solution for torque-free motion as described in the Appendix. A further check on the computational accuracy of the program for torque-free motion is provided by calculating the magnitude of the angular momentum vector H at each time increment and comparing this value with the initial value. Dividing the difference in these values by the initial value gives an indication of the accumulative error. Restricting the difference to less than 0.01% of the initial value assures that the error does not grow too large. Also, the angular momentum vector is evaluated using two different relations, one using the angular velocity $\underline{\omega}$ and the other employing the Euler angles and their time derivatives. Computing the magnitude of the vector difference and restricting it to less than 0.01% of the sum of the magnitudes assures that the defining equations are being satisfied at each increment and that the computational error is small. This latter check is applicable not only for torque-free motion but also for motion with applied moments.

3.0 DYNAMIC BEHAVIOR

The analysis of the dynamic behavior of a vehicle without gyroscopes, as outlined in section 2.5, is now applied to a variety of configurations. The inertial properties of each of the configurations were determined by means of a computer program developed by P. G. Smith [5] which evaluates the principal moments of inertia and the transformation matrix (direction cosines) of the principal axes.

The dynamic behavior of the solar array normal can be described by the Euler angles θ and ψ which relate the body fixed vehicle z-axis to the inertial coordinate system, as shown in Figure 3. The inertial Z-axis is positioned on the sun-line, positive away from the sun. The projection of the inward solar array unit normal, $\underline{r} = (0,0,1)$ onto the inertial X-Y plane is used to display the vehicle dynamics. Its magnitude is $s\theta$, and ψ is the angle between the projection and the negative Y axis. Figure 5 is an example of this display, where specific time values are noted in minutes. This description can also be considered as the trace of the point of intersection of the vehicle z-axis with a unit sphere centered at the origin, as viewed from the inertial Z-axis.

The behavior is studied by means of equations (15) and (23) with the following two sets of initial conditions. In both cases, the body fixed vehicle z-axis (inward solar array normal) is initially positioned slightly off the solar vector ($\theta|_{t=0} = 1^\circ$) in order to avoid computational difficulties in equation (15).

- 1) $\underline{\omega}|_{t=0} = (0,0,\omega_z), \underline{M} = 0, (\theta,\psi,\phi)|_{t=0} = (1^\circ,0,0).$

This is torque-free motion with an angular velocity ω_z about the vehicle z-axis sufficient to attain an artificial gravity level of approximately 0.5 G at the Workshop floor.

- 2) $\underline{\omega}|_{t=0} = 0, \underline{M} = (0,0,M_z), (\theta,\psi,\phi)|_{t=0} = (1^\circ,0,0).$

M_z is the constant applied torque in vehicle coordinates developed by the CSM thrusters about the center of gravity of the Cluster. A 200 pound thrust in the minus y-direction is applied long enough to attain approximately 0.5 G level of artificial gravity at the Workshop floor.

It is also of interest to investigate the loads induced on the components of the Cluster by the motion. In this report, the loads, as described by the force and moment vectors on the hinge joint of one of the Workshop solar arrays, are shown as functions of time. General expressions for the loads on any component are:

$$\begin{aligned}\underline{F}_C &= m_C (\dot{\underline{\omega}} \times \underline{r}_C + \underline{\omega} \times \underline{\omega} \times \underline{r}_C) \\ \underline{M}_j &= \underline{r}_j \times \underline{F}_C\end{aligned}\tag{24}$$

where

\underline{F}_C = force vector acting at the CG of the component

\underline{M}_j = moment vector acting at the joint of the component

m_C = mass of the component

\underline{r}_C = position vector of the component CG with respect to the Cluster CG

\underline{r}_j = position vector of the component CG with respect to the joint of the component

It is shown in the Appendix that the angular velocity and its derivative are periodic functions of time for torque-free motion. Therefore the loads are periodic. For the first set of initial conditions the loads are shown for their first period. In order to make comparison easy, the loads resulting from the second set of initial conditions are also shown for the first period of the torque-free motion which begins when the thrusters are shut off.

The preferred orientation of the angular velocity vector is the vehicle z-axis (normal to the solar arrays) but the actual orientation of the ultimate constant angular velocity of an uncontrolled vehicle with damping is the principal axis of maximum moment of inertia. Thus, the offset angle, α , defined as the angle between the z-axis and this principal axis, will be of major importance, and, as will be demonstrated, the governing parameter in determining the acceptability of a configuration for the artificial gravity experiment.

3.1 Case 1

The first configuration considered is essentially identical to the first Workshop except for added consumables and tanks for its one year mission. Changes in experiments and other modifications will further change the mass and inertia properties of the vehicle, so the following results should be interpreted in a qualitative manner. However, the primary conclusions will certainly remain valid.

For this configuration, shown in Figure 4, the offset angle α has the value 33° . With an assumed spin radius of 36 feet from the vehicle CG to the Workshop floor, an angular velocity of $\omega_z = 6.36$ rpm about the z-axis is required to attain approximately 0.5 G artificial gravity level at the floor (see Figure 1). Assuming the specific impulse of the CSM thrusters is 310 sec., spin-up to 6.36 rpm would take approximately 6 minutes and would consume 418 lbs of fuel.

For the first set of initial conditions, torque-free motion with $\underline{\omega}|_{t=0} = (0, 0, \omega_z)$, the resulting behavior of the vehicle z-axis, as described by $s\theta$ vs ψ , is shown in Figure 5. The amplitude of oscillation of θ is approximately 2α . The vehicle z-axis approximately cones about the axis of maximum principal moment of inertia, while this principal axis approximately cones about the inertial Z-axis. Both cones have a half-angle of α . The force and moment components at the Workshop solar array hinge due to this motion are shown in Figure 6 for one period of their oscillation. The cusp between 0.5 and 0.6 minutes (at $\psi = 1210^\circ$) in Figure 5 corresponds to the end of this period in the torque-free motion. At this point, the angular velocity returns to its initial value but the body-fixed z-axis has not returned to its original position, illustrating that the Euler angles are not periodic functions.

With the second set of initial conditions (constant torque spin-up), the lack of control in the vehicle makes it impossible to attain the required angular velocity. During spin-up the angle θ increases beyond 90° to a maximum of 175° . For such large values of θ the major effect of the applied moment is to change the orientation of the angular momentum vector and not to increase its magnitude, as intended. After 6 minutes of thrusting, the magnitude of the angular momentum H is only 13% of the necessary value. The behavior of the z-axis, beginning at 6 minutes, is shown by the polar plot of $s\theta$ vs ψ in Figure 7; the dashed lines indicate that $\theta > 90^\circ$. These large amplitude oscillations are due primarily to the large value of α and the

lack of control in the vehicle. If control moment gyros were to be used to maintain the first set of initial conditions, they would need a 170,000 ft-lb-sec momentum capability. As the currently available CMGs are rated at 2000 ft-lb-sec each, this type of control is not feasible. If thrusters are considered as a control means, 120,000 ft-lb of torque would be required constantly.

The power output capability of the solar arrays varies approximately linearly with the cosine of the angle between the solar vector and the perpendicular to the arrays. If the vehicle in case 1 is rotated about its axis of maximum principal moment of inertia, and this axis is pointed at the sun, no control would be necessary to maintain constant angular velocity (in the absence of external disturbances), but the power capability of the arrays would be reduced by about 16%. Small changes in the inertia properties of this configuration could increase this power penalty to 75%.

3.2 Case 2

The rather large angular velocity of 6.36 rpm needed to attain an artificial gravity level of 0.5 G in case 1 is due to the comparatively short spin radius of 36 feet from the Cluster CG to the floor of the Workshop. The configuration studied now is one where the spent SII stage remains attached to the Workshop as shown in Figure 8. The CG of this configuration is in the waste tank making the Workshop floor an unsuitable site for the artificial gravity experiment. But if a floor is installed in the Multiple Docking Adapter (which would have only 25% of the floor area of the Workshop) and is used for the artificial gravity experiment, the spin radius is increased to 65 feet and an angular velocity of 4.76 rpm would be required for a 0.5 G artificial gravity level (see Figure 1).

The offset angle α for this case is still quite large and the dynamic behavior is quite similar to that of case 1, shown in Figures 5 and 7. The primary difference between the results is an increase in the length of the period of the oscillatory motion. This is caused by the marked increase in the inertia properties; the maximum moment of inertia is larger than in case 1 by nearly an order of magnitude. The CMG capability required to maintain the constant angular velocity vector parallel with the body-fixed geometric z-axis is also dependent on the inertia properties. It is a function of the products of inertia and is double the value of case 1. The fuel used during spin-up and spin-down operations is not only dependent on the inertia properties but also the angular velocity required and the moment arm of the CSM thrusters (longer in this case because

of the new CG location). However, the order of magnitude increase in inertia overshadows the effects of the other terms and the amount of fuel required for spin-up increases by a factor of three.

These very large inertia terms would also seem to make any existing attitude control system ineffective. Also, because of the location of the center of gravity, the zero-gravity point is unavailable to the crew.

3.3 Case 3

In order to reduce the value of α in case 2, the cross-shaped solar arrays on the ATM are removed. To maintain the power supply capability, the Workshop solar arrays are extended to twice their original size. These modifications reduce α to 22° . So as to generalize this configuration to accommodate either solar or stellar astronomy by the ATM, the ATM experiment package is mounted on a ring gear that surrounds the MDA. This gear is assumed capable of rotating the ATM through an angle γ about the geometric x-axis of the vehicle, where γ is measured from the solar ATM position. This configuration is shown schematically in Figure 9.

As a result of the rotation of the ATM, the inertial properties of the Cluster change and so, too, does the value of α . The offset angle α versus the ATM position angle γ is shown in Figure 10. There are four values of γ for which α reduces to 1.5° or less. If the ring gear were not used, but the ATM mounted permanently at an angle γ that makes $\alpha \sim 1.5^\circ$ or less, options are available for either type of astronomy. For $\gamma \sim 15^\circ$ the ATM would be in a suitable position for solar astronomy; for $\gamma \sim 195^\circ$ stellar astronomy would be most practical; while for $\gamma \sim 77^\circ$ and $\gamma \sim 255^\circ$, it is possible that either solar or stellar astronomy could be accomplished by permitting large angular rotations of the experiment package relative to the ATM structure.

With a reduced value of $\alpha \sim 1.5^\circ$, the CMG capability would still have to be 14,000 ft-lb-sec to hold the angular velocity vector parallel to the geometric z-axis. However, if the vehicle is allowed to spin about the axis of maximum principal moment of inertia, the resulting steady rotation (neglecting external disturbing torques) would require no CMG control. Rotation about this axis imposes a penalty on the solar power of approximately $(1 - \cos\alpha)$ if the axis is directed at the sun.

Figure 10 also shows the limits on the offset angle α for solar power penalties of 1%, 2%, and 3%. So it would seem that positioning the ATM body properly will give satisfactory dynamic behavior with an acceptable loss of solar power. However, as in case 2, there is no zero-gravity location available and the fuel requirement is the same. All of the problems caused by the increased inertia properties are still extant, even with an acceptable value of α .

3.4 Case 4

The fourth configuration is similar to the original configuration of case 1 where the S-II stage is jettisoned. A stellar, rather than solar, ATM is included. Stellar astronomy is accommodated by relocating the ATM solar arrays inboard on the MDA, and the ATM on the plus z-axis 180° from the original location. This modification reduces the offset angle α to 18°, as shown in Figure 11, but the CG location on the x-axis is the same as case 1. Thus the spin radius, angular velocity, and gravity level are all identical to case 1, with the artificial gravity experiment location again at the Workshop floor.

The dynamic behavior of this configuration with the first set of initial conditions (torque-free constant angular velocity) is similar to that of case 1 with the Euler angle θ oscillating with an amplitude of approximately 2α . The motion of the body-fixed z-axis is shown in the $s\theta$ vs ψ polar plot of Figure 12, where the radial scale for $s\theta$ has been changed from that of Figure 5 (case 1) in order to show the details of the motion more clearly.

The loads on the Workshop solar array induced by this motion are pictured in Figure 13 for one period of oscillation. This period is smaller than that of case 1, shown in Figure 6, because of the different inertial properties (the initial conditions are identical). The peak-to-peak amplitude of the periodic loads is less than that of case 1.

Subject to the second set of initial conditions (constant torque spin-up), the behavior of case 4 is much smoother (less wobble) than case 1. During spin-up the Euler angle θ does not increase beyond 40° so the constant applied torque is steadily increasing the magnitude of the angular momentum of the vehicle, not merely changing its orientation. As a consequence, in contrast to case 1, at $t=6$ minutes (when the torque free motion begins), the angular velocity is sufficient to produce an artificial gravity level of approximately 0.5 G. The motion of the body-fixed z-axis is shown in the polar plot of Figure 14, where the radial scale for $s\theta$ has again been changed from case 1.

The loads on the Workshop solar array for one period of torque-free motion after spin-up are shown in Figure 15. Comparison with Figure 13 reveals that the loads have a different profile for the two sets of initial conditions. This is due to the fact that the character of ω at $t=0$ (Figure 13) is not duplicated at $t=6$ minutes (Figure 15), and the torque-free motion depends very strongly on these initial conditions. The period of oscillation, however, depends on the angular momentum, kinetic energy, and inertia properties, and is approximately the same for the two.

In order to control this motion by means of CMGs, equation (15) indicates that for this case, $|\underline{H}_g| = 120,000$ ft-lb-sec which is still far beyond present capabilities. If, however, the vehicle is rotated about the axis of maximum principal moment of inertia to achieve steady motion, the penalty on the solar power supply would be only 5%.

A configuration acceptable for solar astronomy, with the ATM in its original position but the ATM solar arrays remounted on the opposite side of the MDA, will have similar dynamic properties.

3.5 Case 5

Remounting the cross-shaped ATM solar arrays inboard on the MDA on the negative z-axis, as in case 4, but positioning the ATM experiment package 90° from its original position results in the configuration shown in Figure 16. Either solar or stellar astronomy could be accommodated if the ATM experiment package were relocated within the ATM structure. This configuration reduces α to 3.5° and the dynamic behavior of the vehicle is relatively smooth as compared to the previous cases considered. The motion of the z-axis is shown in the $s\theta$ vs ψ polar plot of Figure 17, which again has a different radial scale for $s\theta$. The maximum value of θ under the first set of initial conditions is 8° , still approximately twice the value of α . The loads on the Workshop solar array for one period of the oscillation are shown in Figure 18. The motion has very little wobble and thus the loads approach constant values.

The behavior of this configuration after being spun-up according to the second set of initial conditions is extremely smooth. At $t=6$ minutes the Euler angles are $(\theta, \psi, \phi) = (4, 273, 151)$ degrees and the angular velocity is $\underline{\omega} = (.18, -.31, 6.7)$ rpm. The vehicle z-axis describes an almost perfect cone of about 2° half-angle about an axis which is 3° from the inertial Z-axis.

The θ vs ψ polar plot would appear as a slightly off-center circle which is constantly being repeated. The force components exerted on the Workshop solar arrays by this motion are very nearly constant, varying by only 5 lbs as compared to the variation of 25 lbs in Figure 18 resulting from the first set of initial conditions.

The CMG capability required to align the rotation vector with the geometric body-fixed z-axis of this configuration is about 20,000 ft-lb-sec, which is still too large. But with $\alpha = 3.5^\circ$, the power loss caused by rotating about the axis of maximum principal moment of inertia would be only 0.6%. Thus, constant rotation about this axis would be acceptable.

3.6 Case 6

Reducing the offset angle can be accomplished in many ways, including rearrangement of the internal layout of the Workshop so as to reduce the product of inertia terms I_{xz} and I_{yz} . In case 3 it was shown that rotation of the ATM could reduce α to an acceptably small value at four different positions.

If the S-II stage is jettisoned, case 3 becomes the configuration shown in Figure 19, with the ATM mounted on a ring gear. Again the offset angle α becomes a function of the angle of rotation γ of the ATM, which is shown in Figure 20. There are four values of γ which reduce α to 4° or less. Rotation about the sun-oriented axis of maximum inertia would impose no more than a 1% penalty on array power output.

As in case 3, if the ATM is permanently repositioned and the experiment package is given two degrees of freedom, then solar or stellar astronomy would be feasible.

In order to evaluate the effect of possible changes in the inertial properties, the mass distribution of case 1 was altered so as to produce a new value for α of 70° . Using this new value, case 6 was analyzed again and the α vs γ results are shown in Figure 21. The effect is less qualitative than quantitative in nature and the offset angle α is now more sensitive to positioning of the ATM experiment package, but it is still possible to attain minimum solar power loss for certain values of γ .

3.7 Case 7

Without making any modifications in the positions of the components, the inertial properties of the assembly can be altered by deploying counterweights on booms. In this analysis, the counterweights are treated as point masses with no intrinsic inertial properties. Only their mass and fixed position with respect to the assembly's center of gravity affect the inertial properties of the entire Cluster. The size of a single mass is limited to a maximum of 20 slugs and the length of the boom to 200 feet. In addition, the booms should intersect the spin axis perpendicularly so that the masses will exert only tensile forces on them. As the optimum orientation of the spin vector would be coincident with the body-fixed geometric z-axis, the positions of the ballasting masses are restricted to plus or minus 10 feet from the center of gravity in the z-direction. This restriction assures that the booms can be mounted to the Workshop within its basic diameter.

The first type of ballast considered is composed of symmetric point masses of 20 slugs each located at $(\bar{x}, \bar{y}, \bar{z})$ and $(-\bar{x}, -\bar{y}, -\bar{z})$ with respect to the assembly's center of gravity. For any particular value of \bar{z} , the values of the offset angle α generated by point masses at \bar{x}, \bar{y} form a surface over the \bar{x}, \bar{y} plane. This surface has a "valley" with a nearly constant value of minimum α , occurring when the axis of maximum principal moment of inertia lies in the $\bar{x}\bar{z}$ plane. The minimum value of the offset angle α ($\sim 5^\circ$), is due to the fact that the axis of minimum principal moment of inertia is 5° from the body-fixed geometric x-axis. This is caused primarily by the product of inertia term I_{xz} , which is on the order of 3×10^5 slug ft². With a total mass of 40 slugs and $\bar{z} = 10$ ft, each mass would have to be positioned at $\bar{x} = \pm 750$ ft in order to completely cancel I_{xz} . This minimum of $\alpha \sim 5^\circ$ is, for reasonable boom lengths, an absolute minimum if the ATM is deployed on the minus z-axis. The angular velocity vector cannot therefore be perfectly aligned with the z-axis.

The lines on Figure 22 are the locus of the mass location points which, for different values of \bar{z} , give the minimum α of approximately 5° . It is apparent from Figure 22 that $\bar{z} = -10$ feet is the optimum value for minimum spar length. Figure 23 shows, in more detail, the contours of constant values of α corresponding to symmetric positioning of 20 slugs at $(\bar{x}, \bar{y}, -10')$ and at $(-\bar{x}, -\bar{y}, 10')$.

Smaller masses may be deployed with similar results and Figure 24 shows the minimum $\alpha \sim 5^\circ$ and also $\alpha = 6^\circ$ contours for masses of 10 and 15 slugs placed symmetrically at $(\bar{x}, \bar{y}, -10')$ and $(-\bar{x}, -\bar{y}, 10')$. The 20 slug case is repeated from Figure 23. From this figure, two counterweights of 644 pounds each would require booms approximately 40 feet in length, while less mass, say 483 pounds per counterweight, would require booms about 50 feet long, and two 322 pound counterweights would need 70 foot booms.

Ballasting with non-symmetric positions $(\bar{x}, \bar{y}, -10')$ and $(\bar{x}, -\bar{y}, 10')$ of the 20 slug masses was also considered. As shown in Figure 25, the surface of values of α is of quite different shape than that of Figure 23, though the values for $\bar{x} = 0$ are identical. The minimum boom length for this non-symmetric deployment always occurs when $\bar{x} = 0$. With symmetric deployment, however, shorter boom lengths are possible. This is evident from Figure 24 with \bar{x} given a small negative value for 10 slug masses.

It appears that deployment of ballast masses is a possible way to reduce α , but the problems of precise deployment and the stiffness of the deployment booms must be considered in more detail.

4.0 DISCUSSION

It is apparent that the vehicle dynamical behavior is highly dependent upon the offset angle α , defined as the angle between the geometric, body-fixed z-axis and the axis of maximum principal moment of inertia. The angle α must be small to permit the use of the solar arrays for electrical power. The configurations with the ATM optimally positioned (cases 5 and 6) and with ballast on deployable booms (case 7) reduce α to an acceptable value.

Permanent repositioning of the ATM at a position that gives minimum α might seem at first to be appealing. However, other factors must be considered, primarily, the required changes in the ATM to meet the astronomy objectives. Also the orientation of the axis of maximum principal moment of inertia cannot be precisely predicted before launch. Further, during the mission, leakage, use of consumables, disposal of waste, etc., will be changing the mass and inertia properties of the vehicle. However, rotation of the position of the ATM about the geometric x-axis has a great deal of control over α . The configuration in case 6 where the ATM solar arrays are incorporated in the Workshop solar

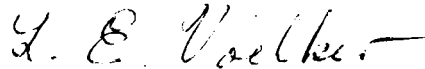
arrays and the ATM body is mounted on a ring gear would appear to be the most versatile of all considered. It has the capability of minimizing the effects of the indeterminate changes in mass or inertia properties by in-flight change in the position of the ATM. The ring gear could also provide one of the two degrees of freedom of the ATM, relative to the Workshop, that are needed for stellar astronomy.

Factors which were not considered in this investigation but which are felt to be of importance and require further study for the artificial gravity experiment include the following:

1. Provision of an internal, passive damping system in order to:
 - a) reduce the wobble (oscillatory motion) of the spin axis during spin-up
 - b) align the angular velocity and angular momentum vectors with the axis of maximum principal moment of inertia
 - c) reduce the effects of perturbations due to crew motion, changes in mass and inertia properties, external influences, etc.
2. An analysis of the internal dissipation of energy due to the hysteresis effect of the oscillatory loads as an aid to 1a, b, c.
3. A thorough investigation of the external influences of
 - a) gravity gradient torques
 - b) aerodynamic torques
4. The elastic response of some of the components to structural loads induced by the dynamic behavior.
5. An attitude control system that will maintain a constant angular velocity about the sun-line despite
 - a) external torques
 - b) changes in mass and inertia properties
 - c) an approximate one degree per day rotation of the sun-line during the 30-day artificial gravity experiment.

5.0 CONCLUSIONS

If solar power is to be used during the artificial gravity experiment, the offset angle α between the geometric z-axis and the axis of maximum principal moment of inertia must be reduced. It must be reduced to such an extent that rotation about this principal axis will not impose too great a penalty on the power output of the solar arrays. Minimization of α will require major modifications, internal and/or external, or possibly some sort of inertial ballasting.



1022-LEV-cf

L. E. Voelker

Attachment
Appendix

REFERENCES

1. Thompson, A. B., "Physiological Design Criteria for Artificial Gravity Environments in Manned Space Systems" in "The Role of the Vestibular Organs in the Exploration of Space," NASA-SP-77, Washington, D.C., 1965.
2. Hoffman, D. B., and McGaughy, R. E., "Centrifugally Obtained Artificial Gravity," Bellcomm Technical Report TR-69-730-1, Washington, D.C., April, 1969.
3. Newsome, B. D., and Brady, J. F., "Observations on Subjects Exposed to Prolonged Rotation in a Space Station Simulation," in "The Role of the Vestibular Organs in the Exploration of Space," NASA-SP-77, Washington, D.C., 1965.
4. Anderson, G. M., "Stellar ATM and Artificial Gravity Meetings - Trip Report," Memorandum for File, Bellcomm, Inc., Washington, D.C., October, 1969.
5. Smith, P. G., "AAP-1/AAP-2 Configuration Data for Solar Orientation Implementation Studies," Memorandum for File, Bellcomm, Inc., Washington, D.C., August, 1967.

APPENDIX

Torque-free Rotational Motion of a Rigid Body *

The equation of motion of a rigid body rotating about its center of gravity in body-fixed coordinates is

$$I \dot{\underline{\omega}} + \underline{\omega} \times I \underline{\omega} = 0 \quad (A-1)$$

where

I = the inertia tensor

$\underline{\omega}$ = the angular velocity vector

$(\dot{})$ = the derivative with respect to time

We may choose the body-fixed coordinate axes to be the axes of principal moments of inertia (I_1 , I_2 , and I_3) so the inertia tensor is diagonal. We can further label the principal moments of inertia such that $I_1 \geq I_2 \geq I_3$.

Equation (A-1) can then be written in scalar form as

$$I_1 \dot{\omega}_1 = (I_2 - I_3) \omega_2 \omega_3 \quad (A-2a)$$

$$I_2 \dot{\omega}_2 = (I_3 - I_1) \omega_1 \omega_3 \quad (A-2b)$$

$$I_3 \dot{\omega}_3 = (I_1 - I_2) \omega_1 \omega_2 \quad (A-2c)$$

where ω_1 , ω_2 , and ω_3 are the components of angular velocity about the principal axes. In order for a non-symmetric body (I_1 , I_2 , I_3 all distinct) to undergo steady rotation about an axis, $\dot{\underline{\omega}} \equiv 0$ and equations (A-2) become

$$\omega_1 \omega_2 = \omega_2 \omega_3 = \omega_1 \omega_3 = 0 \quad (A-3)$$

*This analysis is included for the sake of completeness. Similar derivations are listed in the Appendix bibliography.

A non-trivial solution exists if one and only one component of angular velocity is non-zero. Thus, steady rotational motion about an axis is possible only if it is a principal axis.

In order to solve equations (A-2) for general (non-steady) rotational motion we now write expressions for twice the kinetic energy T and the square of the magnitude of the angular momentum vector H .

$$2T = I_1\omega_1^2 + I_2\omega_2^2 + I_3\omega_3^2 \quad (\text{A-4})$$

$$H^2 = (I_1\omega_1)^2 + (I_2\omega_2)^2 + (I_3\omega_3)^2 \quad (\text{A-5})$$

Both T and H remain constant during torque-free motion if there is no internal energy dissipation. From (A-4) and (A-5) we can write expressions for ω_1 and ω_3 in terms of ω_2 ,

$$\omega_1^2 = C_1 - C_2\omega_2^2 \quad (\text{A-6a})$$

$$\omega_3^2 = C_3 - C_4\omega_2^2 \quad (\text{A-6b})$$

where

$$C_1 = \frac{(2I_3T - H^2)}{I_1(I_3 - I_1)} \quad (\text{A-7a})$$

$$C_2 = \frac{I_2(I_2 - I_3)}{I_1(I_1 - I_3)} \quad (\text{A-7b})$$

$$C_3 = \frac{(2I_1T - H^2)}{I_3(I_1 - I_3)} \quad (\text{A-7c})$$

$$C_4 = \frac{I_2(I_2 - I_1)}{I_3(I_3 - I_1)} \quad (\text{A-7d})$$

Squaring both sides of (A-2b) and substituting (A-6), we have

$$(\dot{\omega}_2)^2 = \left(\frac{I_3 - I_1}{I_2} \right)^2 (C_1 - C_2 \omega_2^2) (C_3 - C_4 \omega_2^2) \quad (\text{A-8})$$

With the proper transformations, equation (A-8) can be written in the form

$$\left(\frac{dy}{dx} \right)^2 = (1-y^2) (1-k^2 y^2) \quad (\text{A-9})$$

where $y = \frac{\omega_2}{b}$, $x = pt$, and b and p are chosen such that $0 < k < 1$. The parameters b , p , and k are functions of I_1 , I_2 , I_3 , T and H . Equation (A-9) can be integrated to give

$$x = \int_0^y \frac{dy}{\sqrt{1-y^2} \sqrt{1-k^2 y^2}} \quad (\text{A-10})$$

This is the form of an elliptic integral that has a periodic solution called the Jacobian elliptic function

$$y = \text{sn}(x), \quad \text{sn}(0) = 0 \quad (\text{A-11})$$

with a period of $4K$, where

$$K = \int_0^1 \frac{dy}{\sqrt{1-y^2} \sqrt{1-k^2 y^2}} \quad (\text{A-12})$$

We may define other elliptic functions as

$$\text{cn}(x) = \sqrt{1 - \text{sn}^2(x)} \quad (\text{A-13a})$$

$$\text{dn}(x) = \sqrt{1 - k^2 \text{sn}^2(x)} \quad (\text{A-13b})$$

The similarity between the elliptic functions $\text{sn}(x)$ and $\text{cn}(x)$ and the circular (trigonometric) functions $\sin(x)$ and $\cos(x)$ can be seen by allowing k to go to zero. Equation (A-9) then becomes

$$\left(\frac{dy}{dx} \right)^2 = (1-y^2) \quad (\text{A-14})$$

with the solution

$$y = \sin(x), \quad \sin(0) = 0 \quad (\text{A-15})$$

and the following relations hold:

$$\text{sn}(x) \Big|_{k=0} = \sin(x) \quad (\text{A-16a})$$

$$\text{cn}(x) \Big|_{k=0} = \cos(x) \quad (\text{A-16b})$$

$$\text{dn}(x) \Big|_{k=0} = 1 \quad (\text{A-16c})$$

Using these elliptic functions, the solution to equation (A-8) may be determined.

From (A-4) and (A-5), it follows that $2I_1 T - H^2 > 0$ and $2I_3 T - H^2 < 0$. The components of angular velocity depend upon the sign of the term $H^2 - 2I_2 T$. If this term is positive,

$$\omega_1 = a_1 \operatorname{dn}(pt) \quad (\text{A-17a})$$

$$\omega_2 = a_2 \operatorname{sn}(pt) \quad (\text{A-17b})$$

$$\omega_3 = a_3 \operatorname{cn}(pt) \quad (\text{A-17c})$$

where

$$a_1^2 = C_1, \quad a_2^2 = C_3/C_4, \quad a_3 = -\sqrt{C_3} \quad (\text{A-18a,b,c})$$

$$p^2 = (H^2 - 2TI_3) (I_1 - I_2) / I_1 I_2 I_3 \quad (\text{A-18d})$$

$$k^2 = (I_2 - I_3) (2TI_1 - H^2) / (I_1 - I_2) (H^2 - 2TI_3) \quad (\text{A-18e})$$

If the term $H^2 - 2I_2 T$ is negative,

$$\omega_1 = a_1 \operatorname{cn}(pt) \quad (\text{A-19a})$$

$$\omega_2 = a_2 \operatorname{sn}(pt) \quad (\text{A-19b})$$

$$\omega_3 = a_3 \operatorname{dn}(pt) \quad (\text{A-19c})$$

where

$$a_1^2 = C_1, \quad a_2^2 = C_1/C_2, \quad a_3 = -\sqrt{C_3} \quad (\text{A-20a,b,c})$$

For further details on the mathematics of Jacobian Elliptic Function, see sections 13.1 and 14.1 of Synge and Griffith, "Principles of Mechanics," McGraw-Hill, 1959.

If there is any energy-absorbing mechanism in the body, such as viscous damping or structural hysteresis, then the periodic solutions given by equations (A-17) or (A-19) will eventually be damped out and the motion will be steady ($\dot{\omega}=0$). As shown above, this implies that the angular velocity vector lies on an axis of principal moment of inertia. Because of the energy-absorbing mechanism, the final stable motion will be steady rotation about that principal axis which makes the kinetic energy a minimum. The angular momentum, however, will remain constant as there are no external moments applied.

The kinetic energy T for rotation about a principal axis x_i with an angular velocity ω_i is, by equation (A-4),

$$T = I_i \omega_i^2 / 2 \quad (\text{A-21})$$

and the magnitude of angular momentum H is, by equation (A-5),

$$H = I_i \omega_i \quad (\text{A-22})$$

thus the kinetic energy can be rewritten as

$$T = H^2 / 2I_i \quad (\text{A-23})$$

and, as the angular momentum remains constant, steady rotation about the axis of maximum principal moment of inertia has the minimum kinetic energy.

APPENDIX BIBLIOGRAPHY

1. Arnold, R. N. and Maunder, L., Gyrodynamics and Its Engineering Applications, New York, Academic Press, 1961, 113-122.
2. Bradbury, T. C., Theoretical Mechanics, New York, Wiley, 1968, 229-232, 450-454.
3. Landau, L. D. and Lifshitz, E. M., Mechanics, New York, Pergammon Press, 1960, 116-120.
4. MacMillan, W. D., Dynamics of Rigid Bodies, New York, Dover Press, 1960, 192-196.
5. Routh, E. J., Dynamics of a System of Rigid Bodies, New York, Dover, 1955, 86-88.
6. Synge, J. L. and Griffith, B. A., Principles of Mechanics, New York, McGraw Hill, 2nd ed., 1949, 364-370, 418-425; 3rd ed., 1959, 327-333, 374-380.

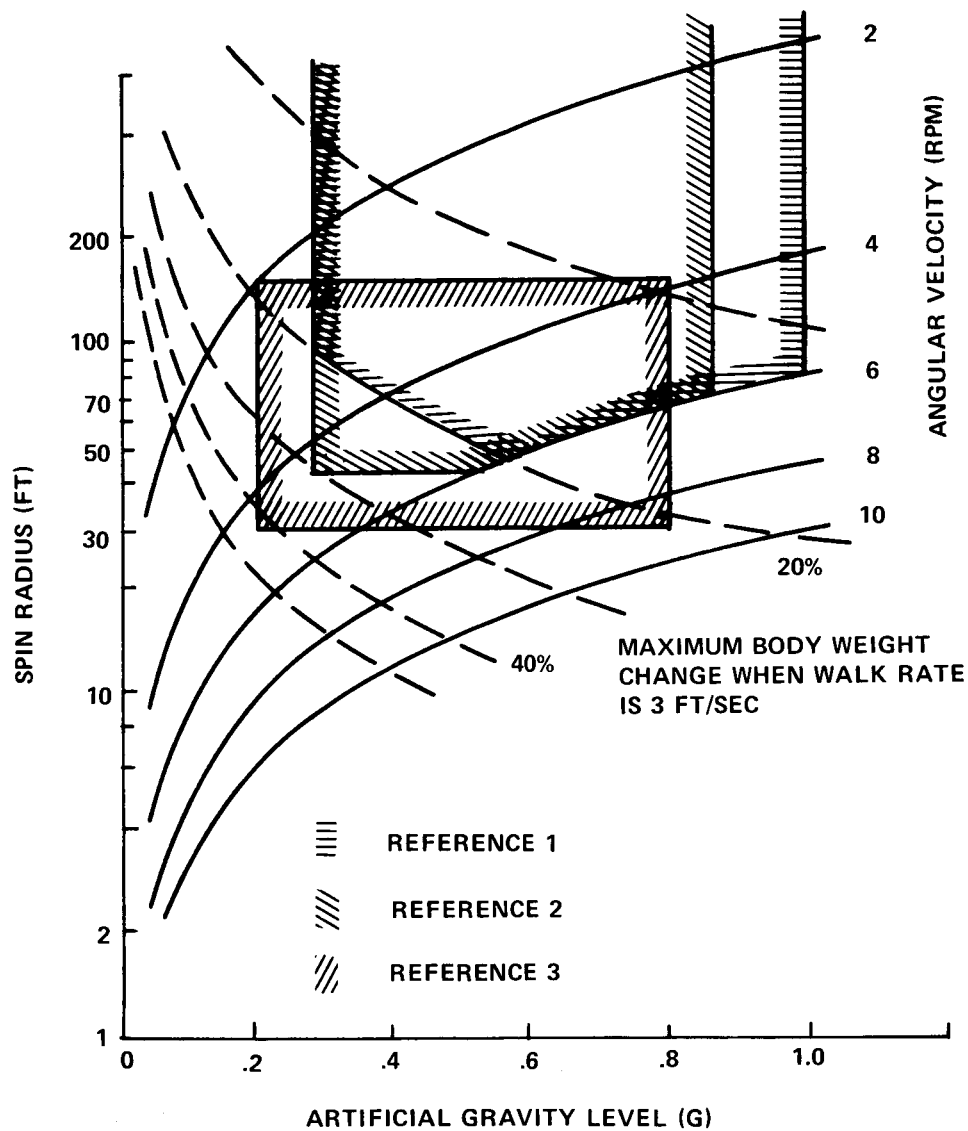


FIGURE 1 - DESIGN CRITERIA FOR ARTIFICIAL GRAVITY

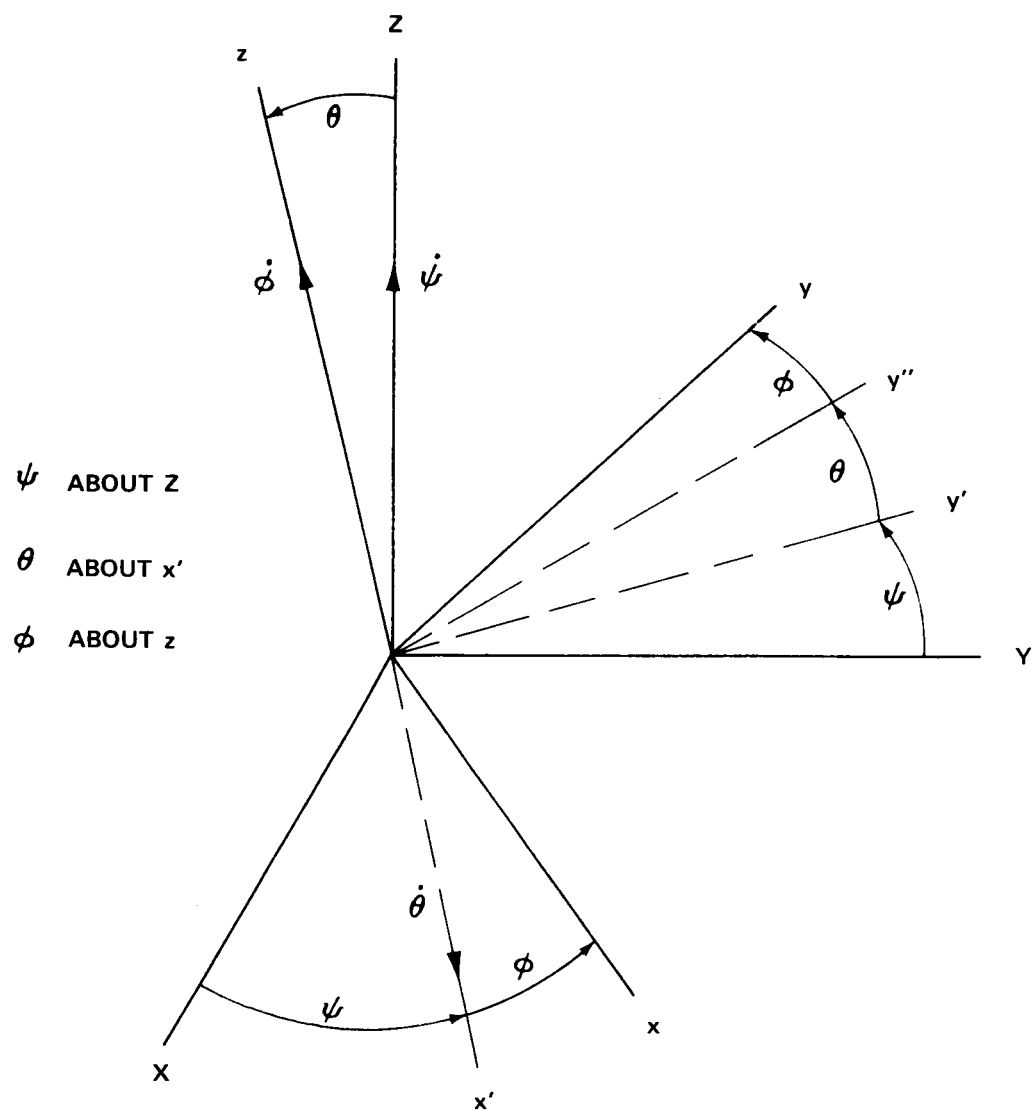


FIGURE 2 - DEFINITION OF THE EULER ANGLES

SUN-LINE

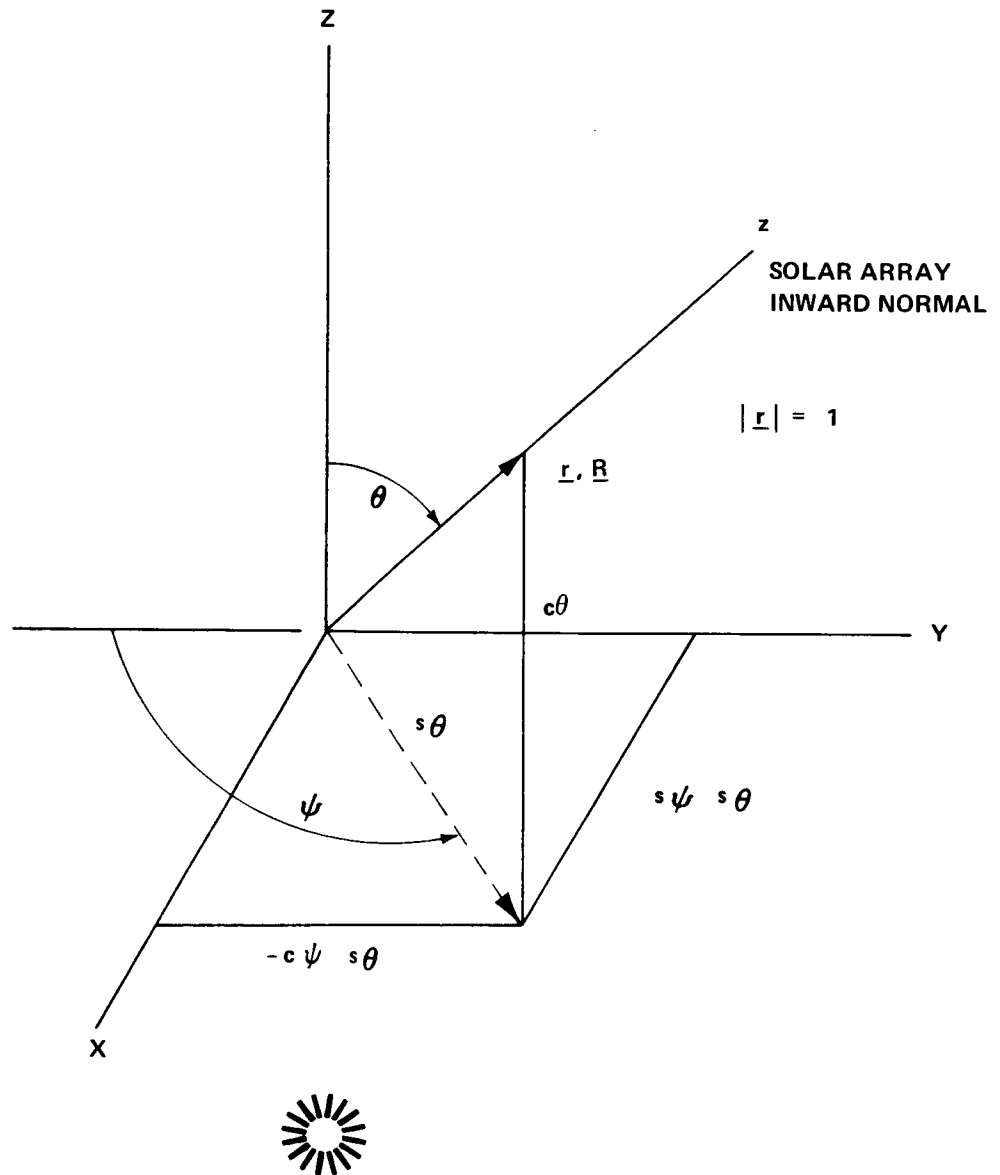


FIGURE 3 - THE BODY-FIXED z -AXIS IN THE INERTIAL COORDINATE SYSTEM

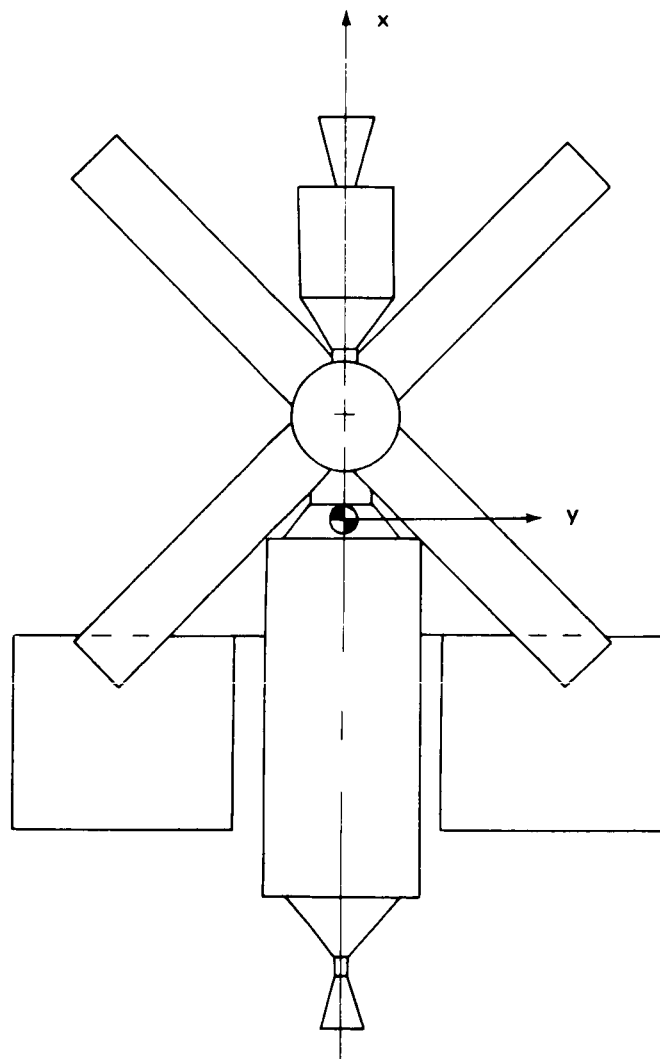
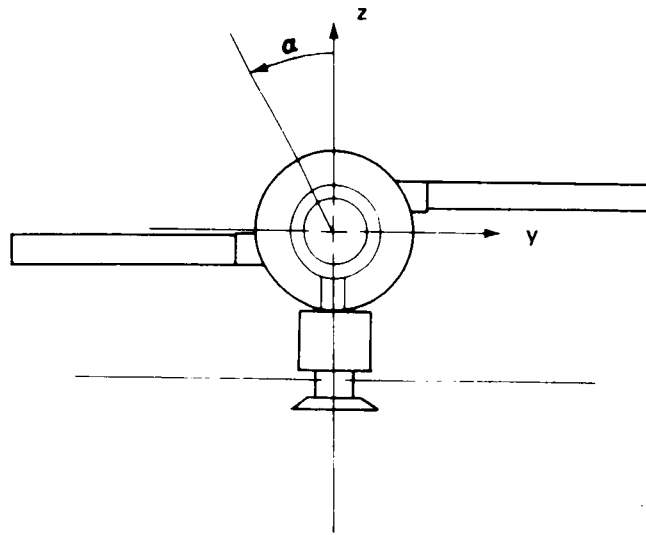


FIGURE 4 - CASE 1: SATURN WORKSHOP AUGMENTED FOR ONE YEAR MISSION

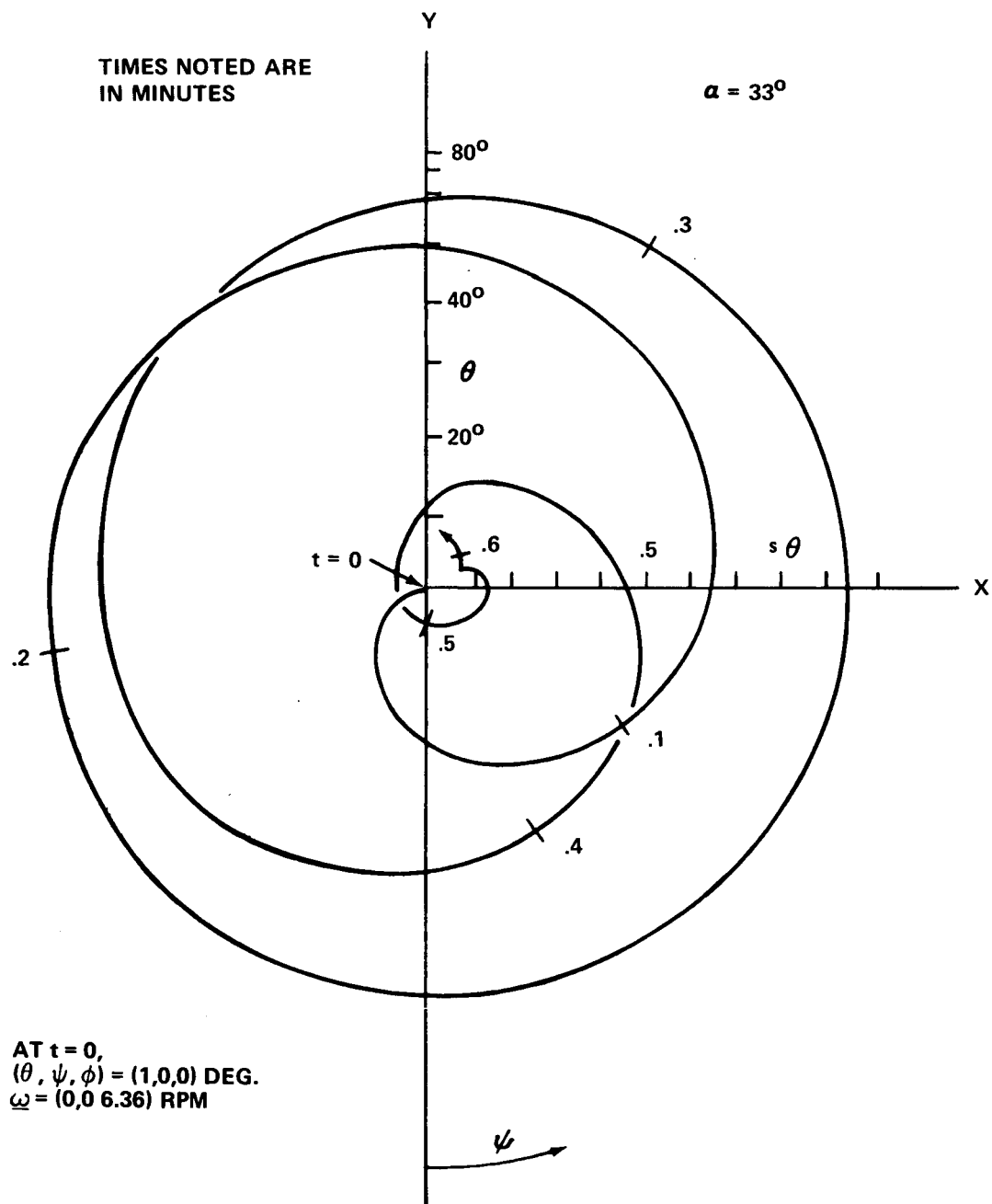
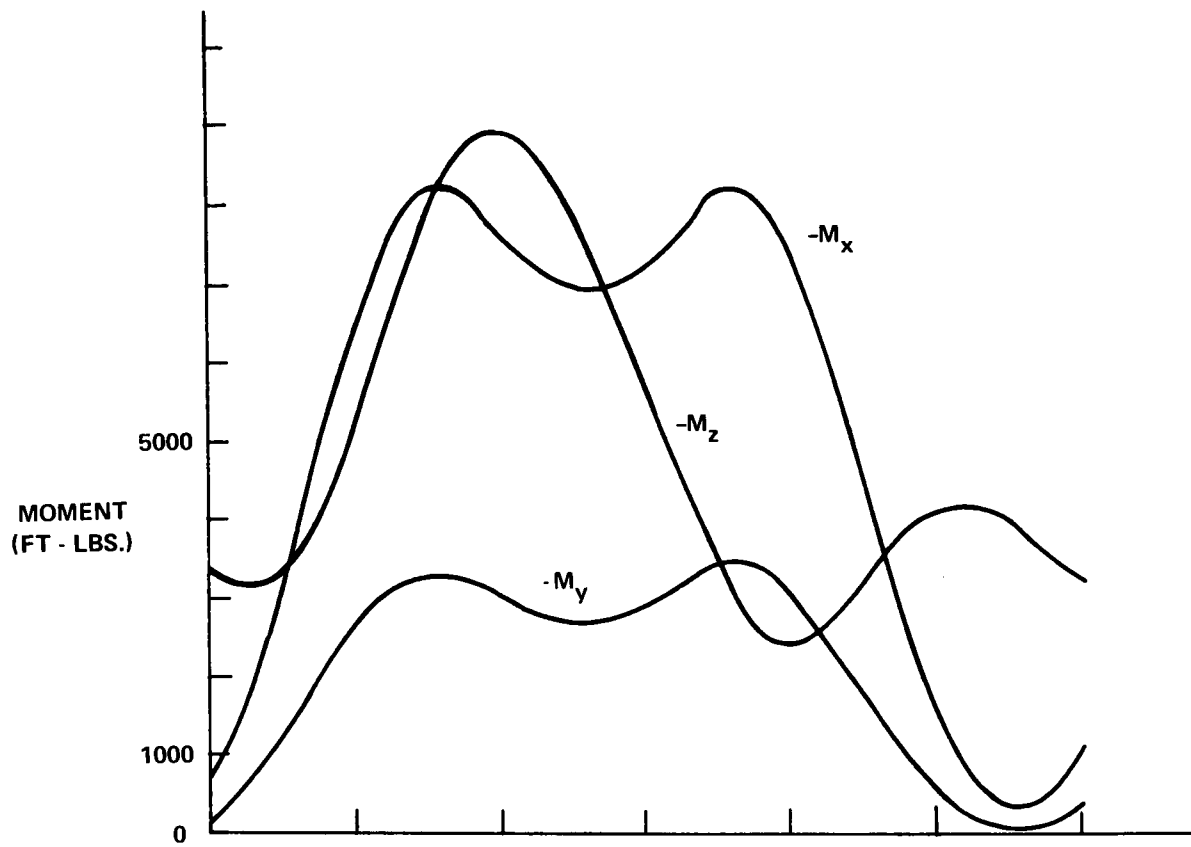


FIGURE 5 - BEHAVIOR OF VEHICLE z-AXIS FOR CASE 1, INITIALLY SPINNING



$\alpha = 33^\circ$

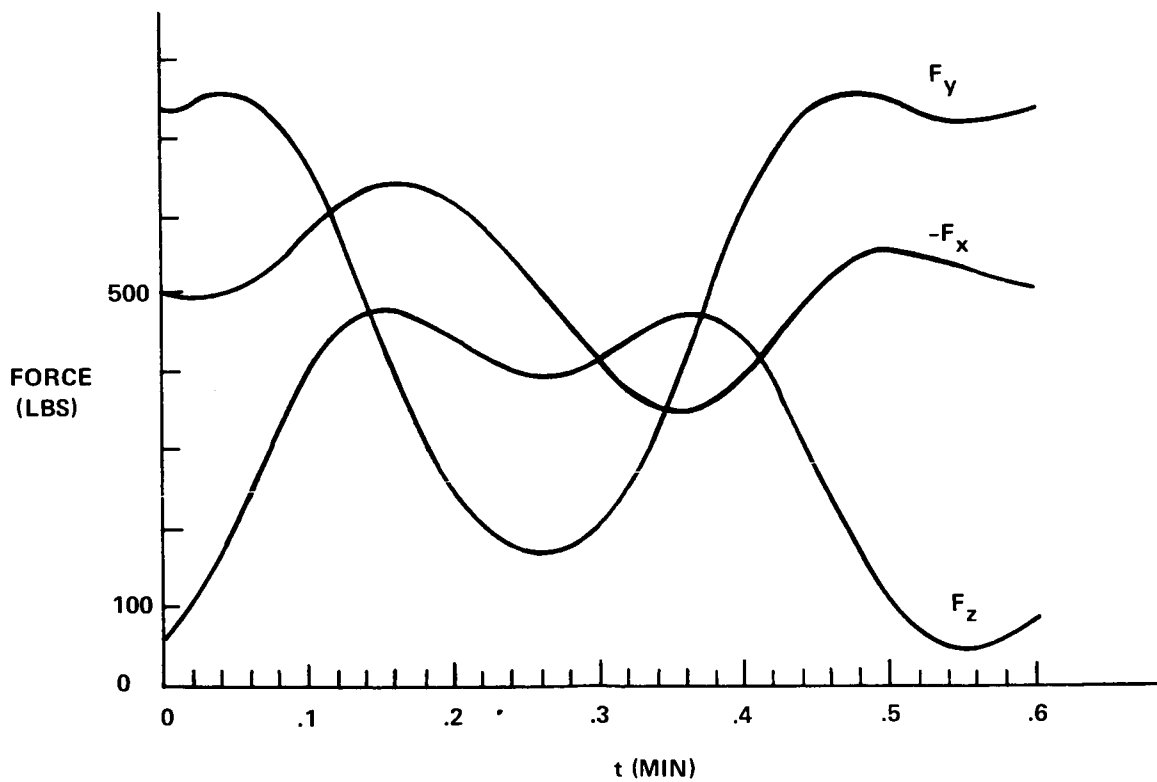


FIGURE 6 - FORCE AND MOMENT COMPONENTS ON THE WORKSHOP SOLAR ARRAY HINGE OF CASE 1, INITIALLY SPINNING

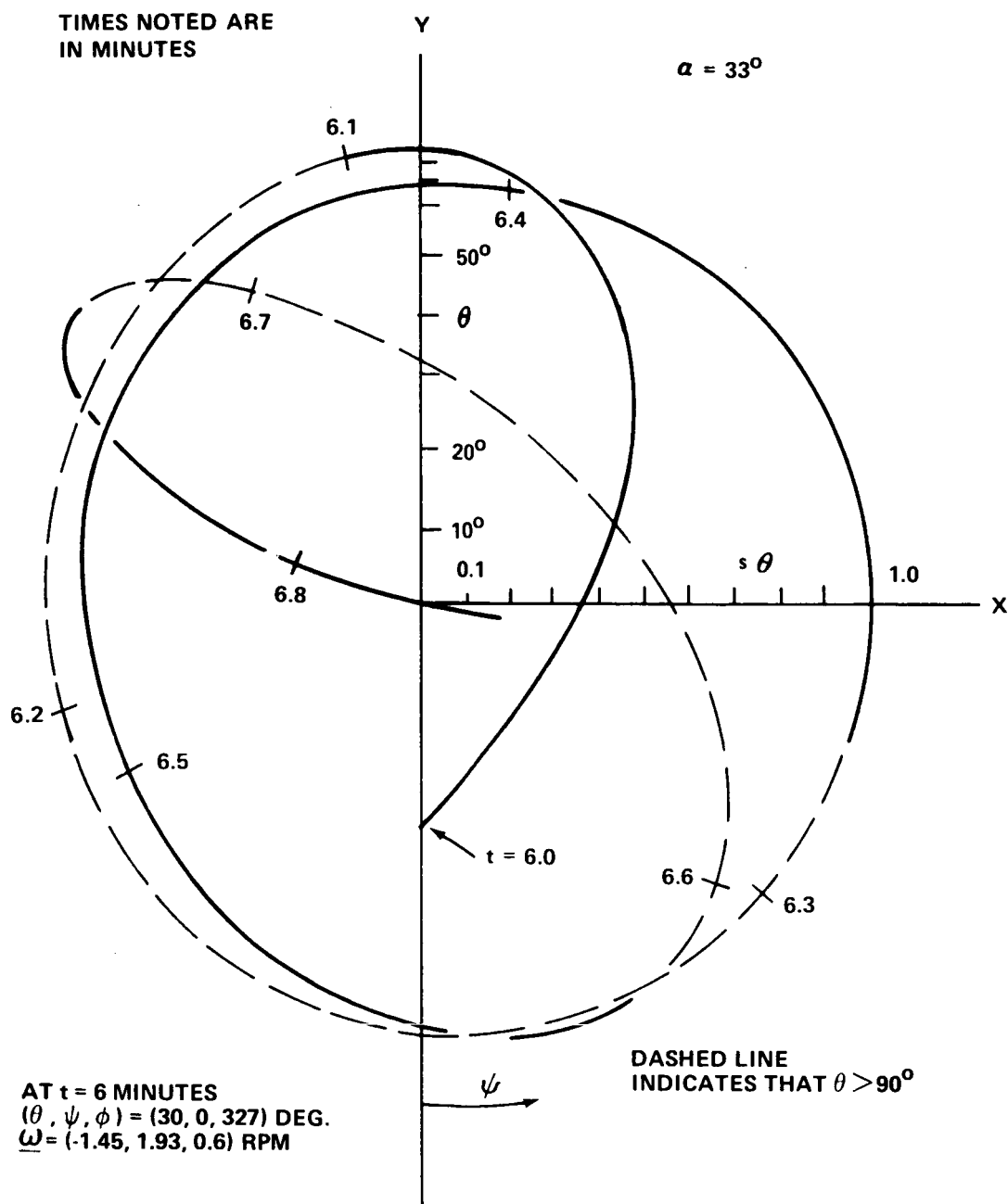


FIGURE 7 - BEHAVIOR OF VEHICLE z-AXIS FOR CASE 1 IMMEDIATELY AFTER SPIN-UP

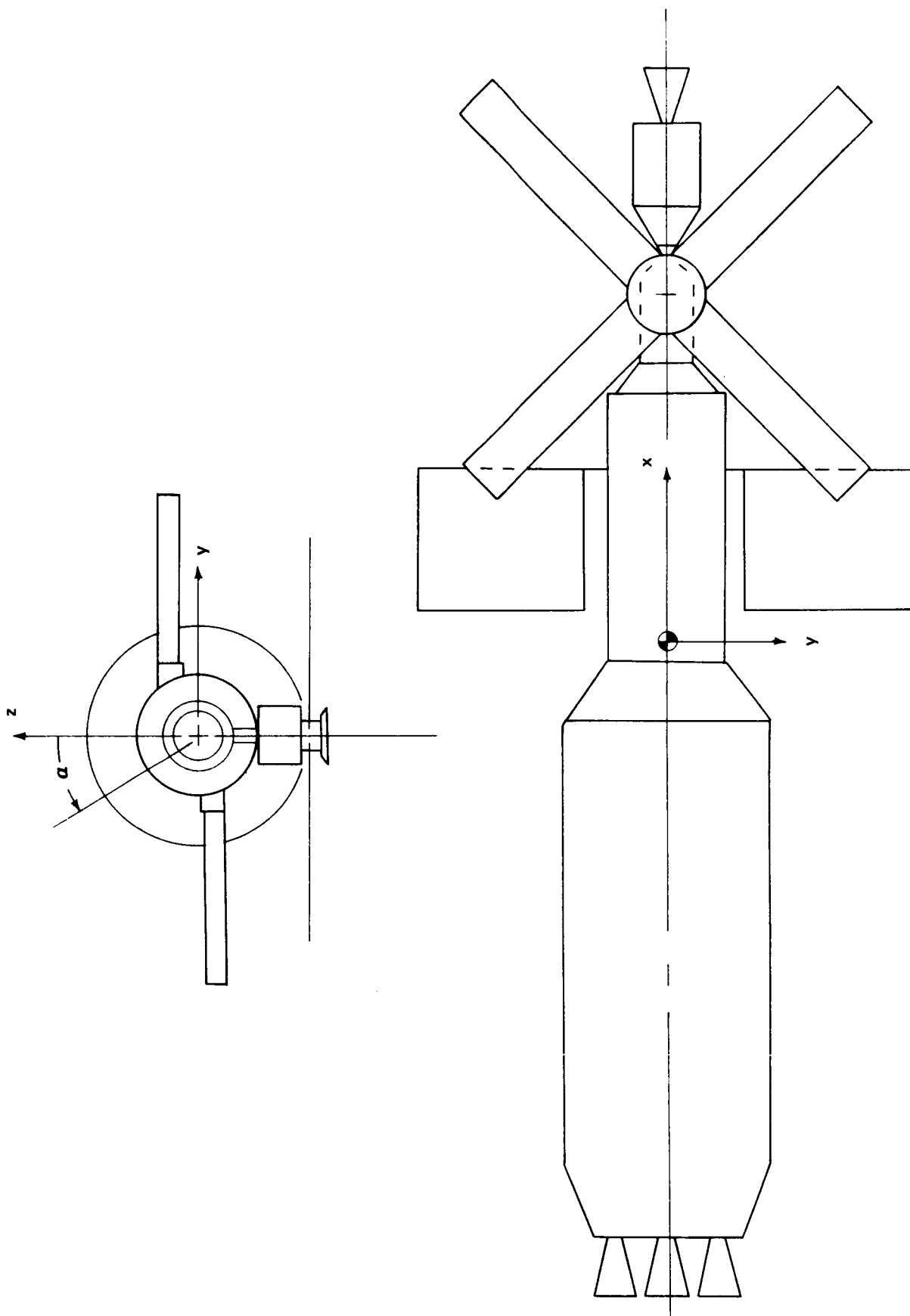


FIGURE 8 - CASE 2: WORKSHOP WITH S-II STAGE ATTACHED

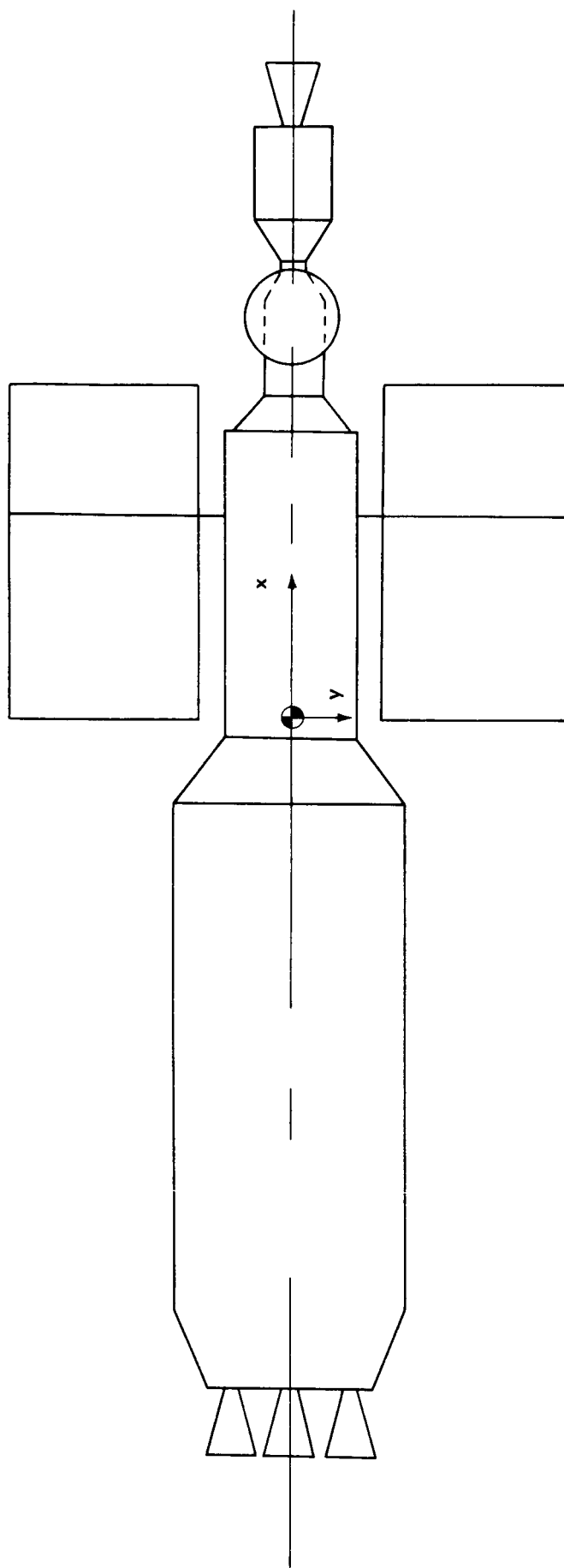
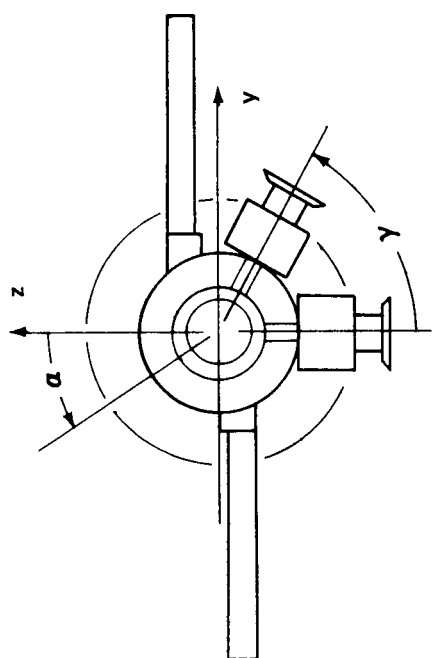


FIGURE 9 - CASE 3: WORKSHOP AND S-II WITH ATM ON RING GEAR, ATM ARRAYS ADDED TO WORKSHOP ARRAYS

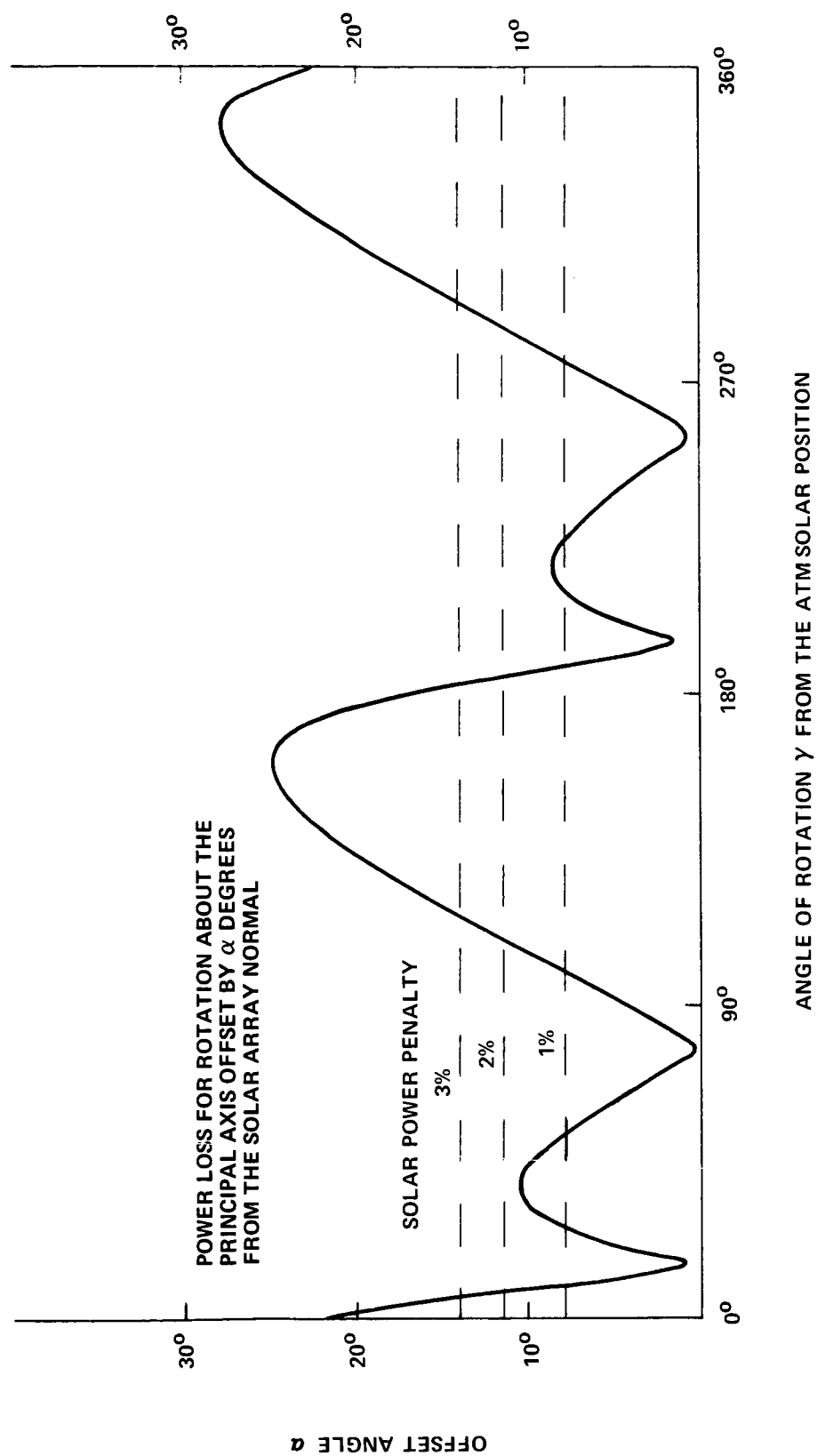


FIGURE 10 - THE OFFSET ANGLE α VS. POSITION OF THE ATM FOR CASE 3.

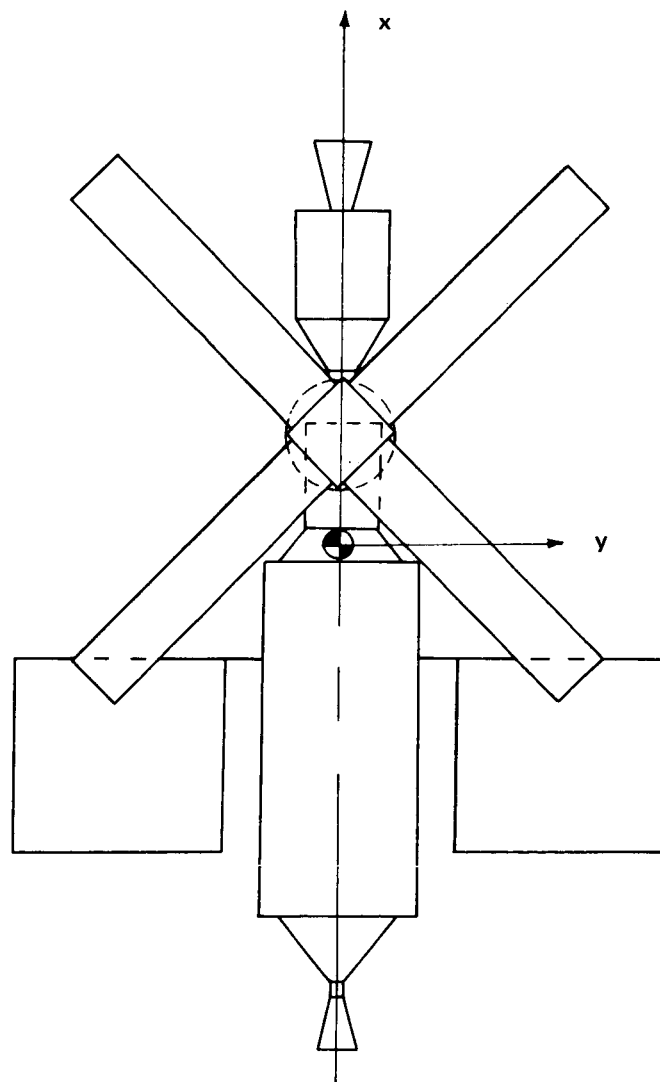
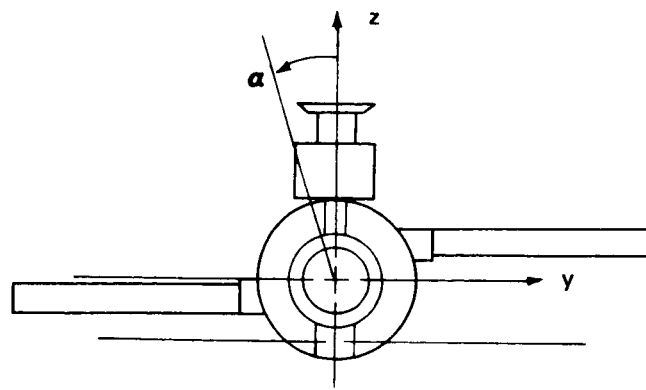


FIGURE 11 - CASE 4: WORKSHOP WITH STELLAR ATM ON POSITIVE z -AXIS AND ATM ARRAYS INBOARD

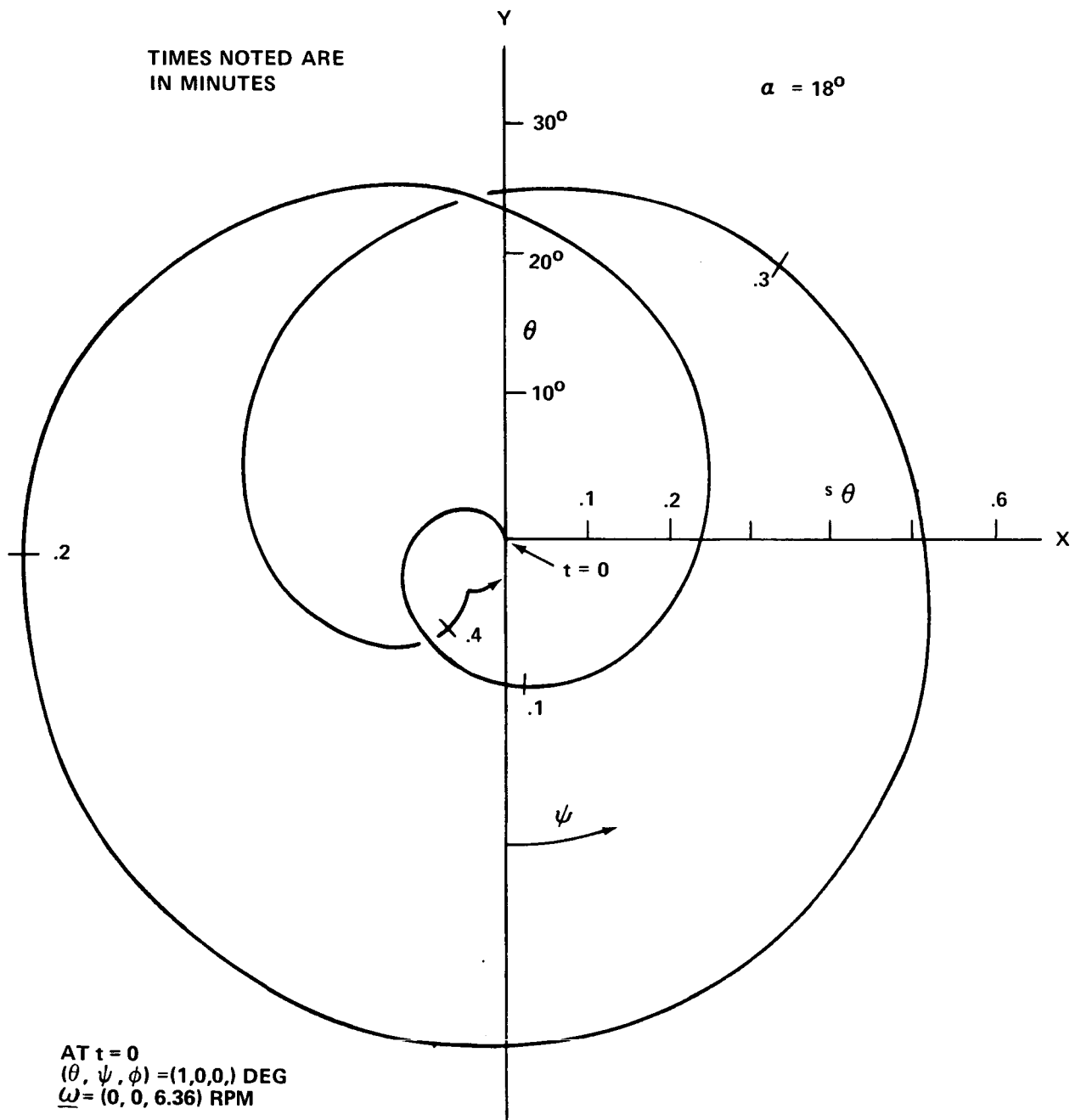


FIGURE 12 - BEHAVIOR OF VEHICLE z-AXIS FOR CASE 4, INITIALLY SPINNING

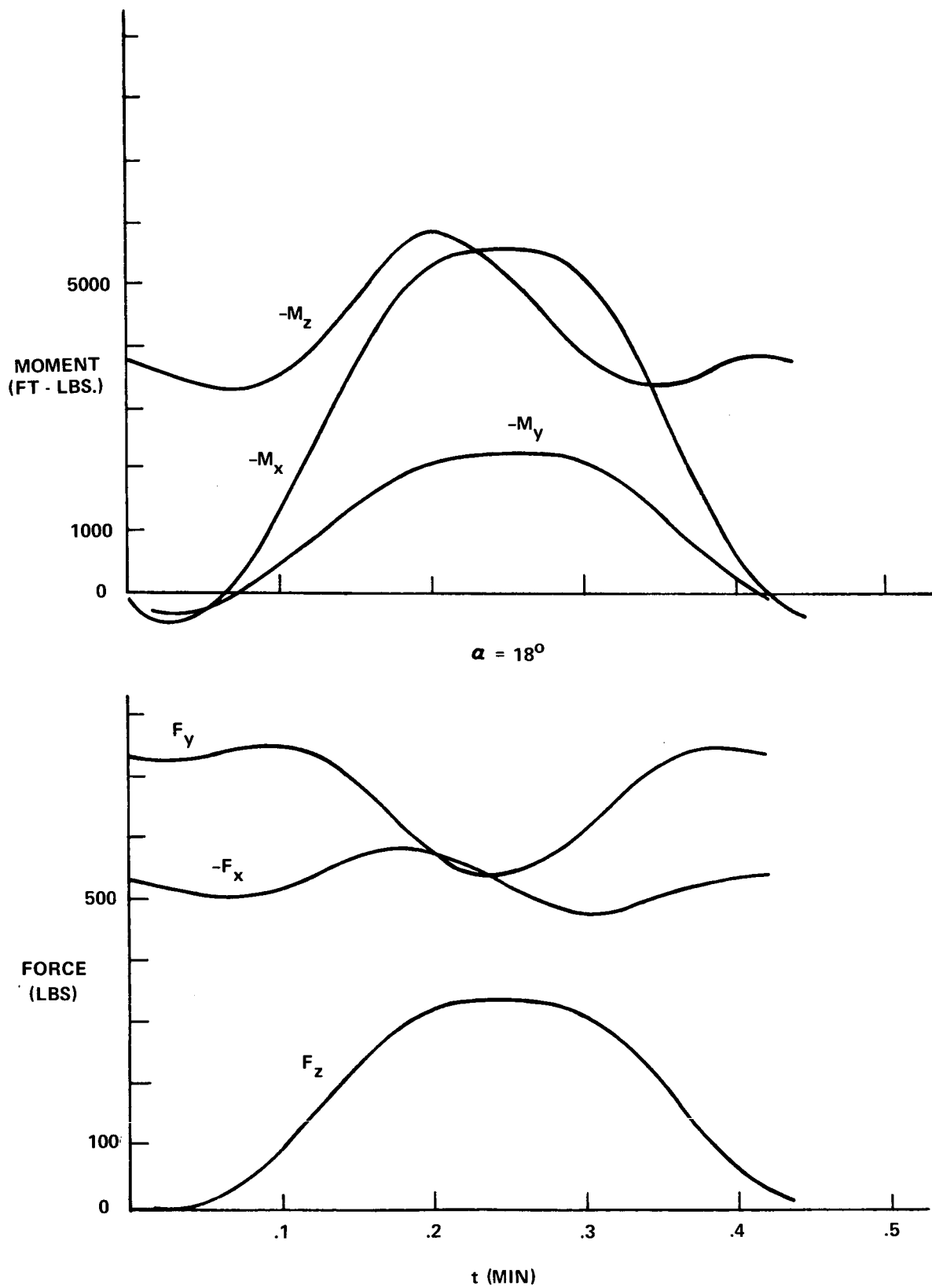


FIGURE 13 - FORCE AND MOMENT COMPONENTS ON THE WORKSHOP SOLAR ARRAY HINGE OF CASE 4, INITIALLY SPINNING

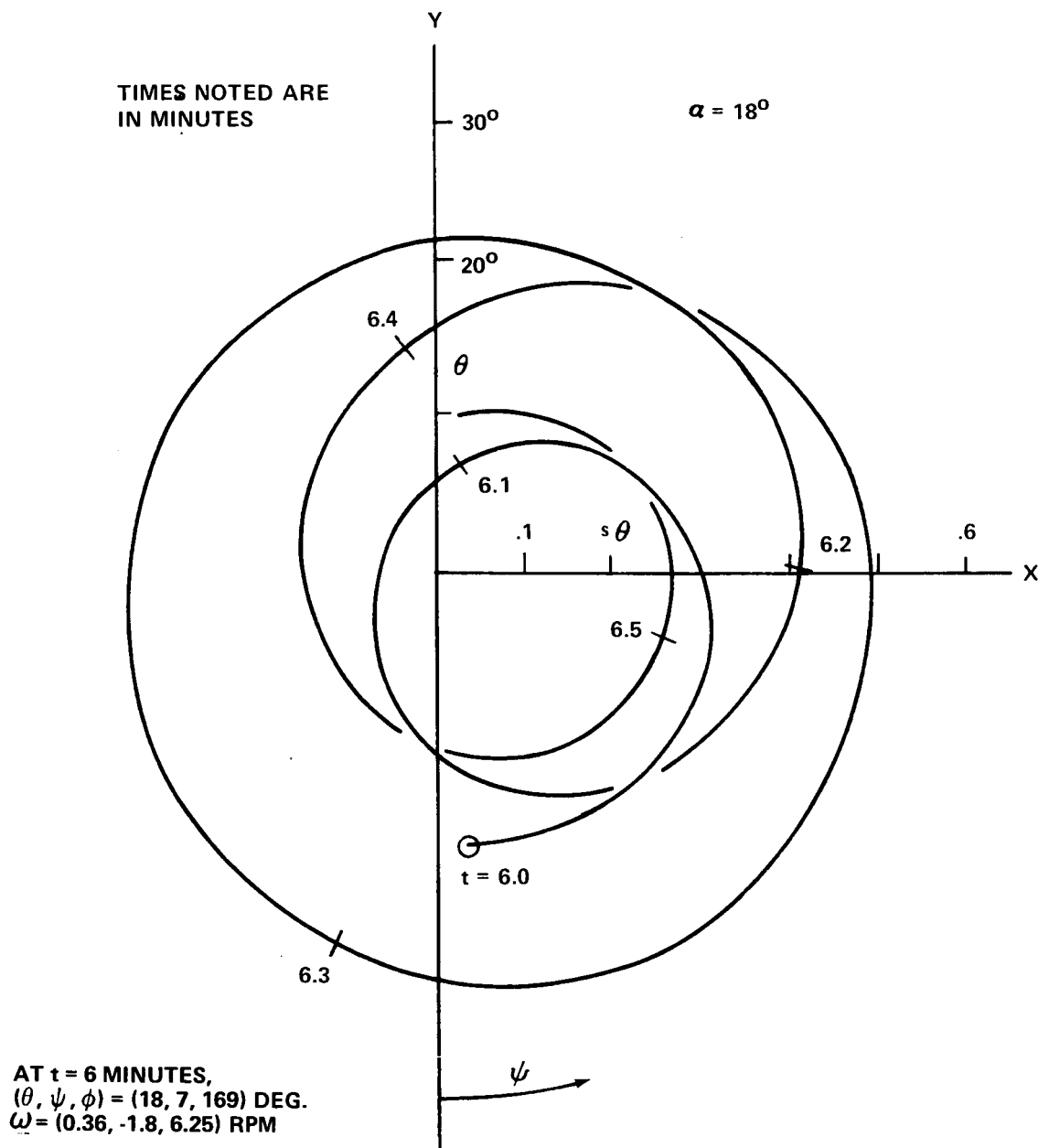


FIGURE 14 - BEHAVIOR OF VEHICLE z-AXIS FOR CASE 4, IMMEDIATELY AFTER SPIN-UP

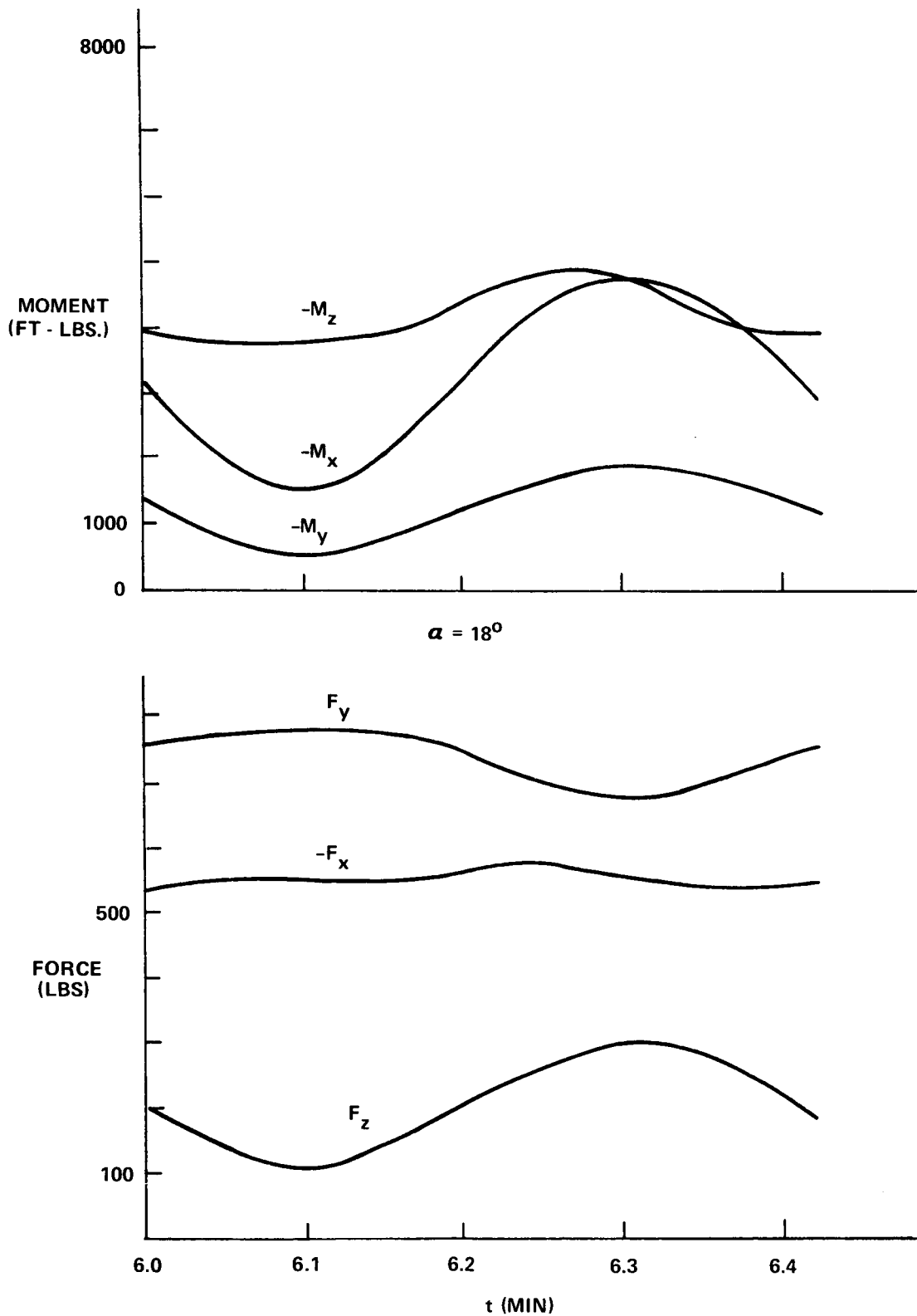


FIGURE 15 - FORCE AND MOMENT COMPONENTS ON THE WORKSHOP SOLAR
ARRAY HINGE OF CASE 4, IMMEDIATELY AFTER SPIN-UP

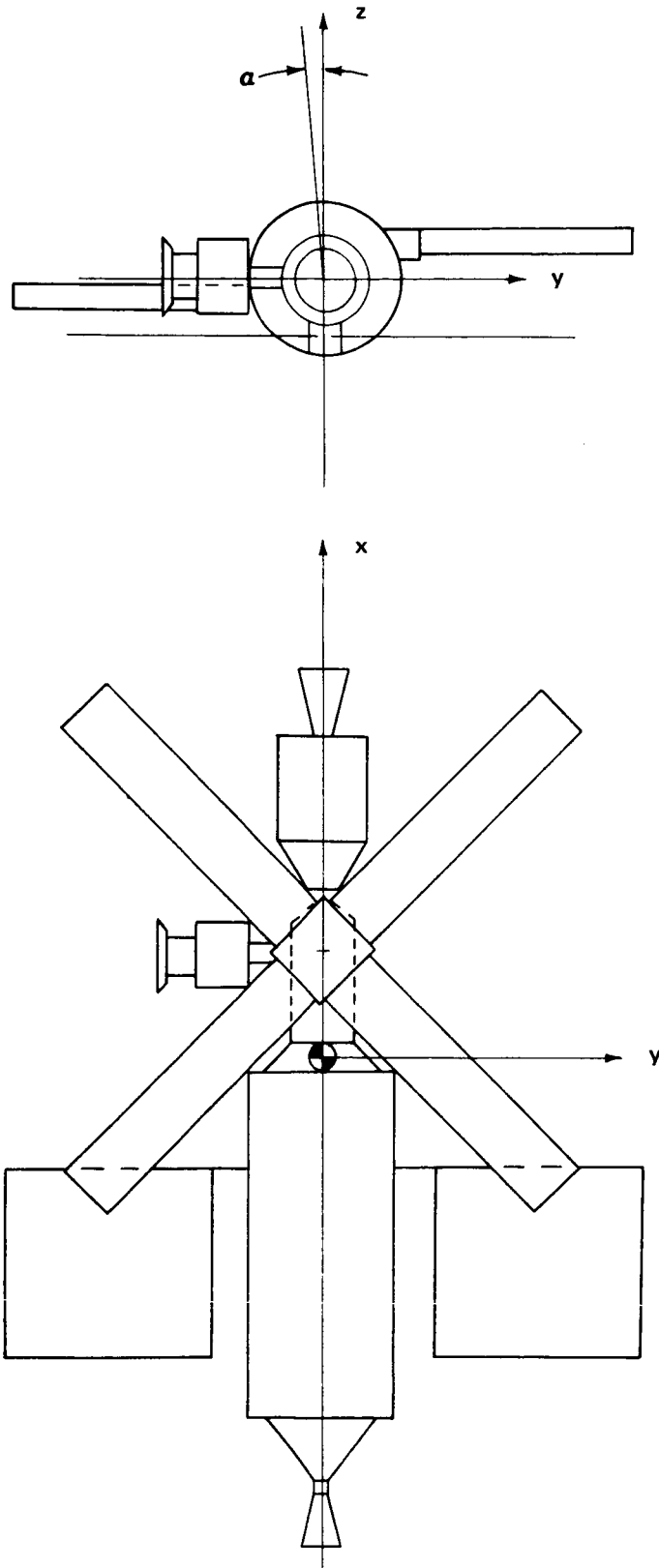


FIGURE 16 - CASE 5: WORKSHOP WITH ATM ON NEGATIVE y -AXIS AND ATM ARRAY INBOARD

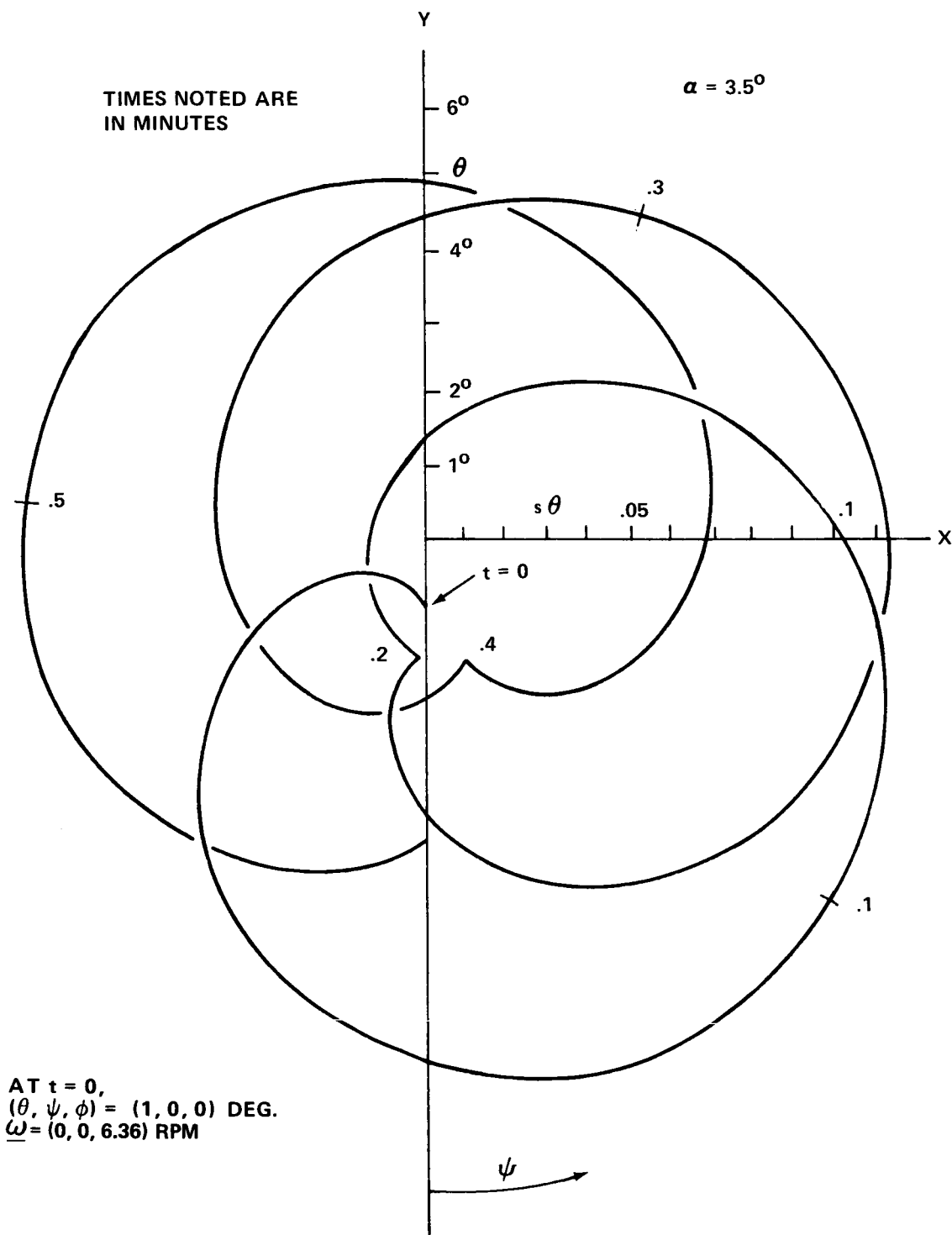


FIGURE 17 - BEHAVIOR OF VEHICLE z -AXIS FOR CASE 5, INITIALLY SPINNING

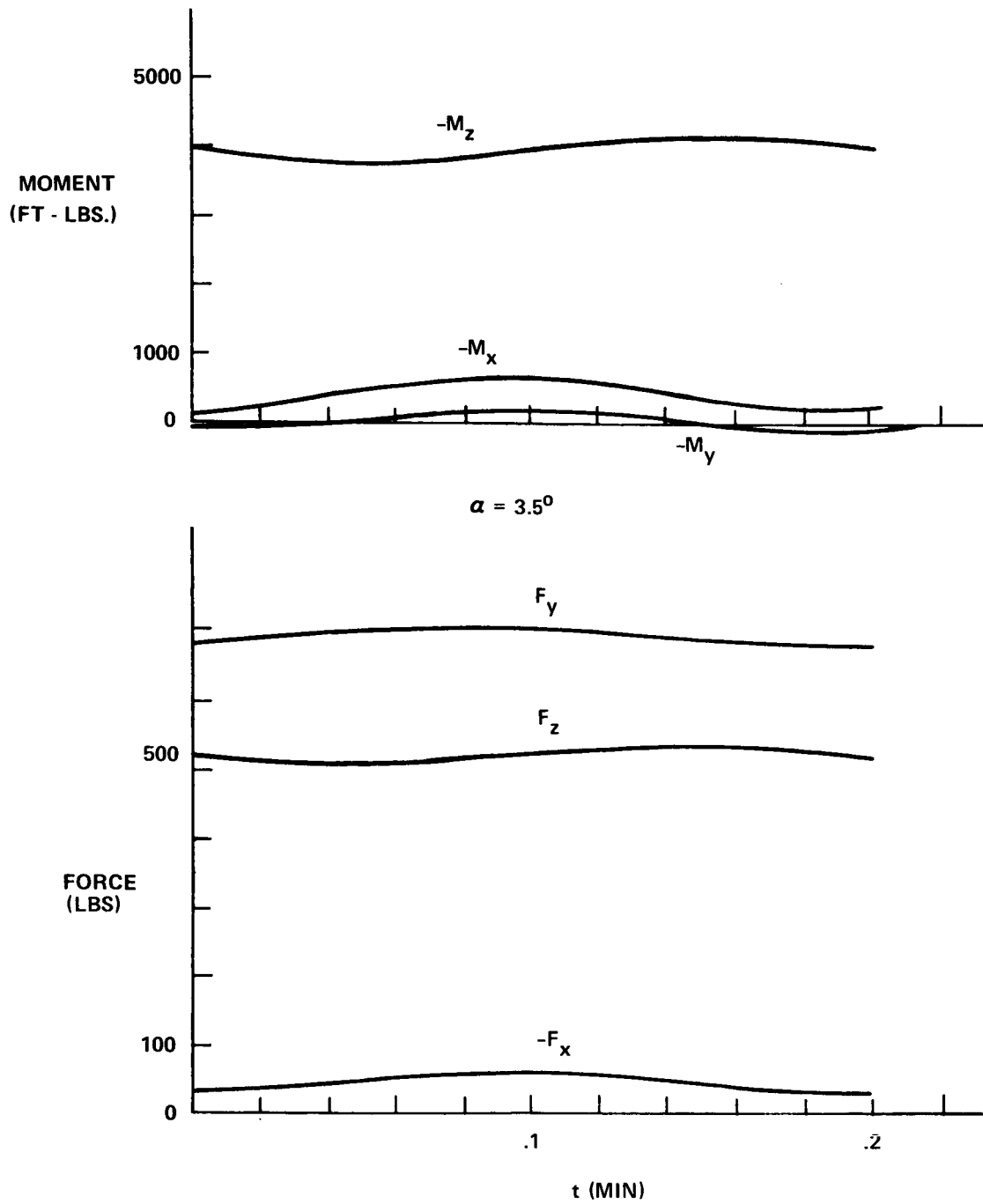


FIGURE 18 - FORCE AND MOMENT COMPONENTS ON THE WORKSHOP SOLAR ARRAY HINGE OF CASE 5, INITIALLY SPINNING

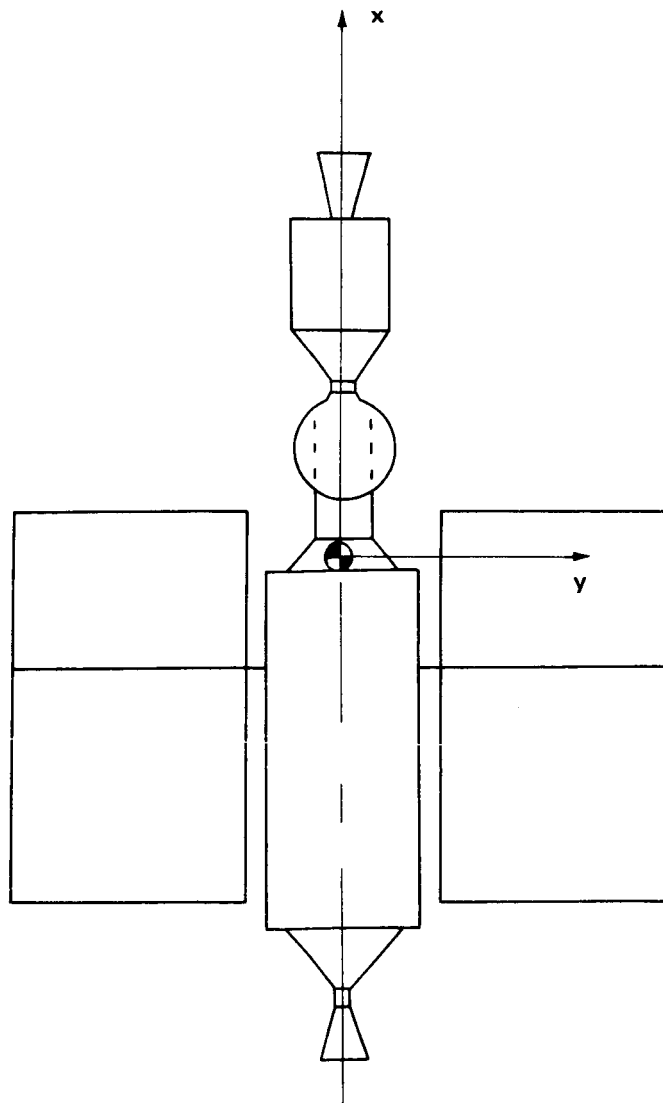
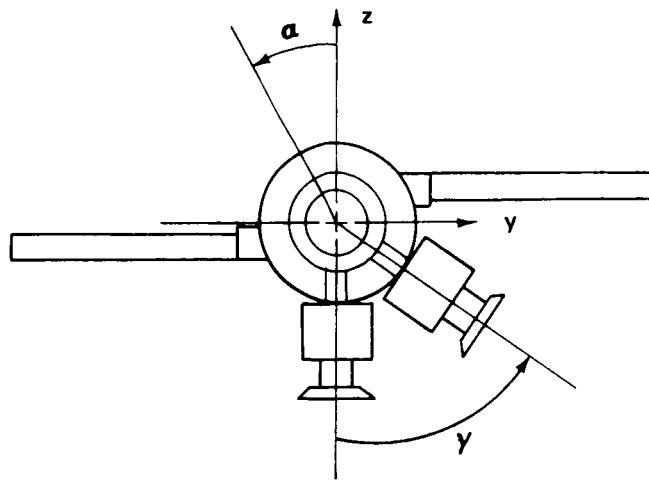


FIGURE 19 - CASE 6: WORKSHOP WITH ATM ON RING GEAR, ATM ARRAYS ADDED TO WORKSHOP ARRAYS

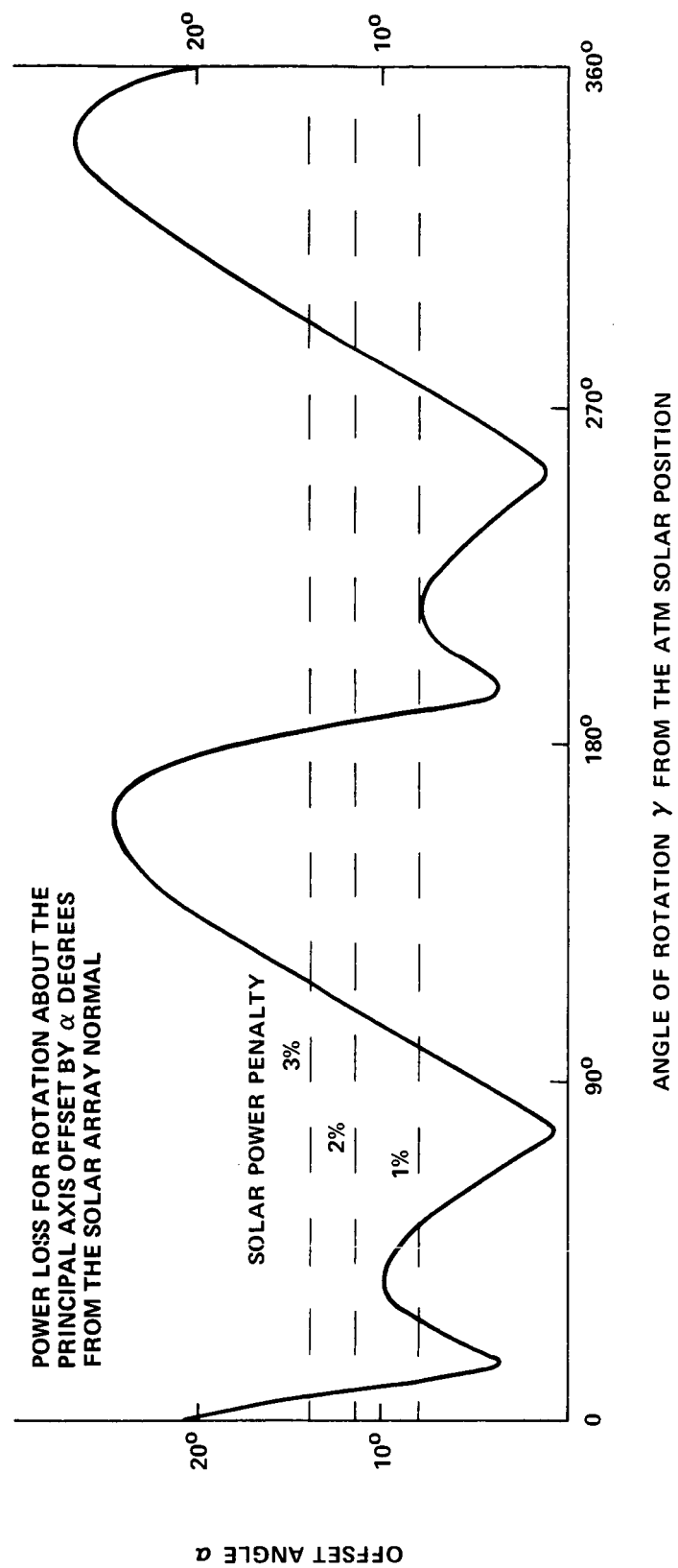


FIGURE 20 - THE OFFSET ANGLE α VS. POSITION OF THE ATM FOR CASE 6

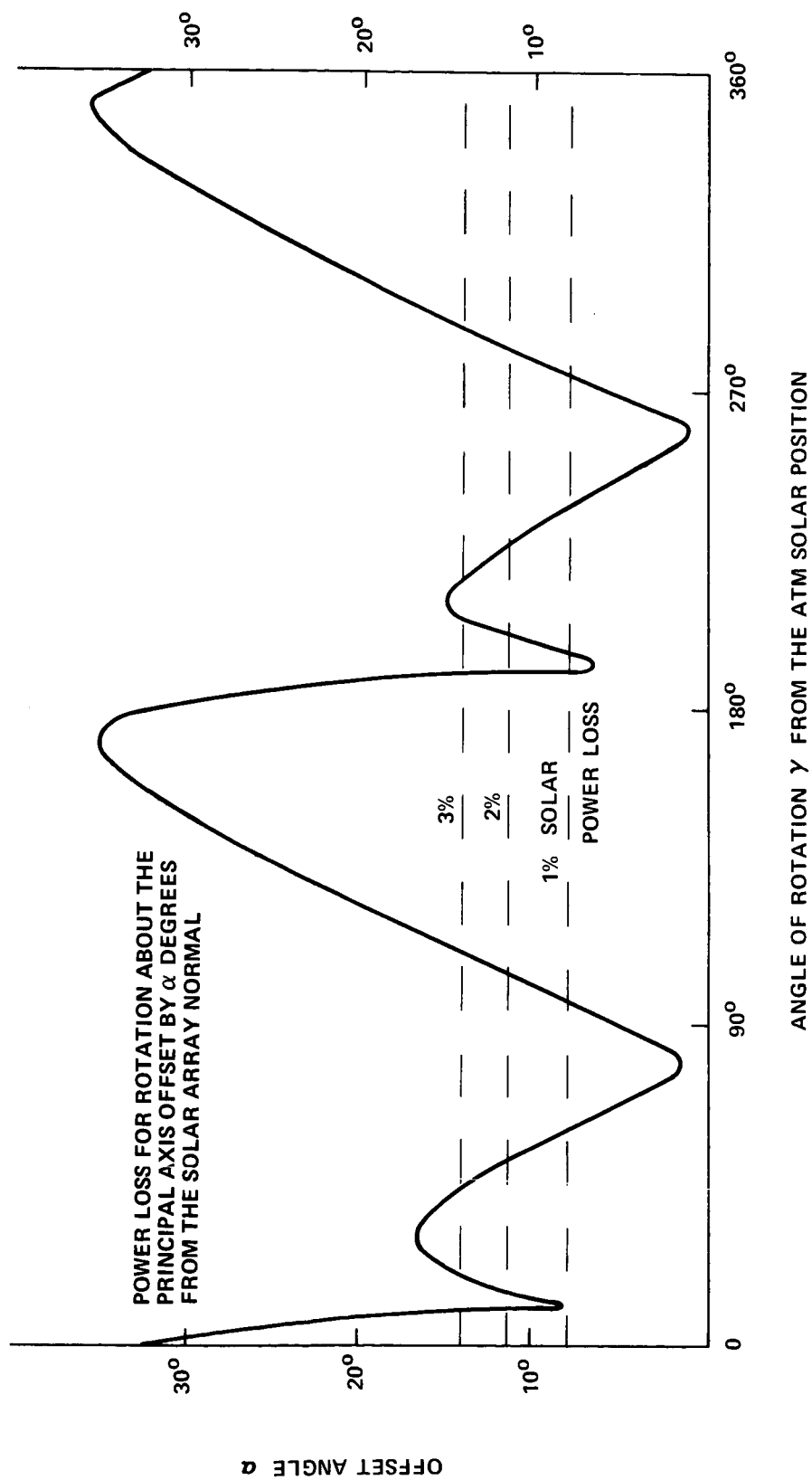


FIGURE 21 - THE OFFSET ANGLE α VS. POSITION OF THE ATM FOR CASE 6 WITH ALTERED INERTIA PROPERTIES

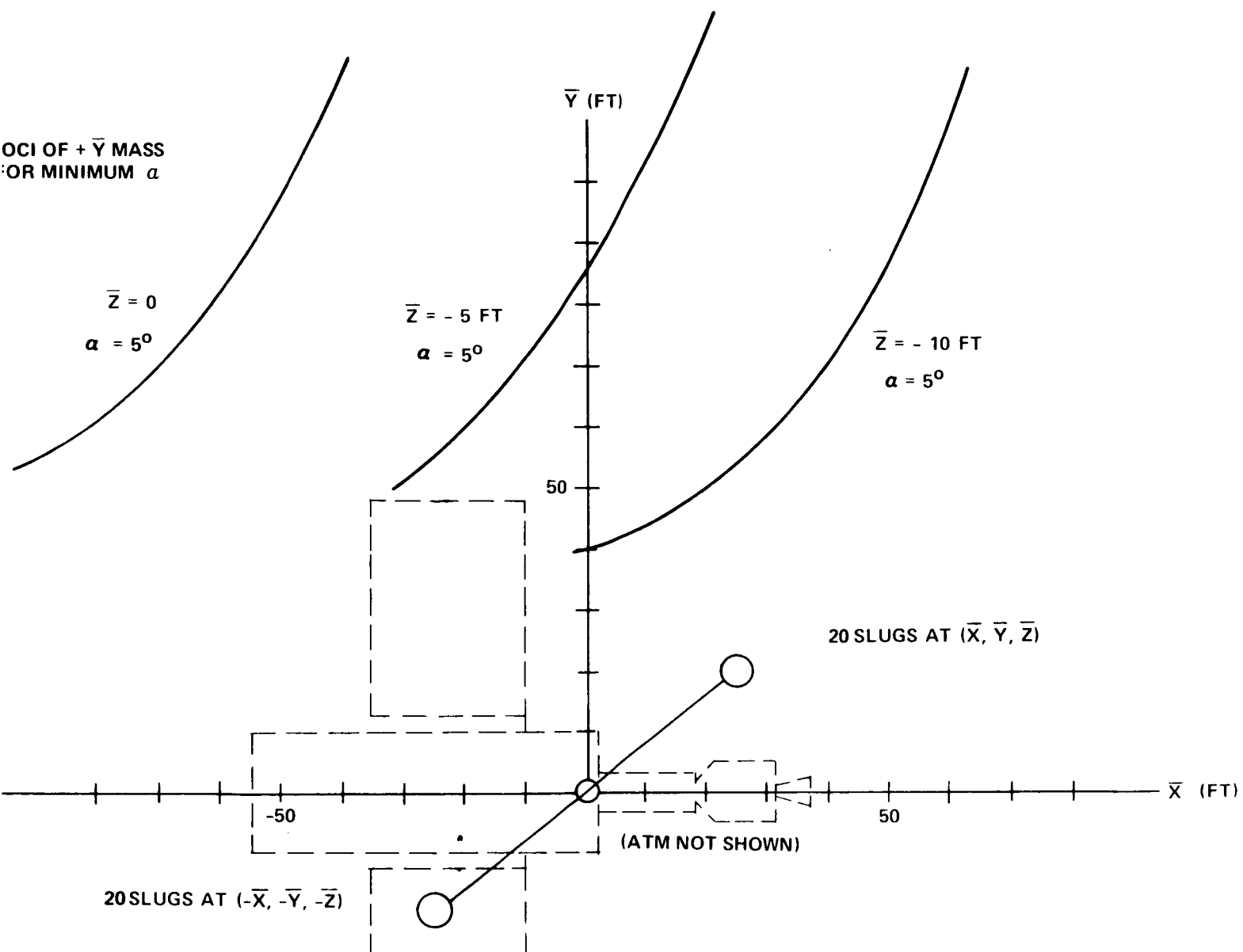


FIGURE 22 - THE EFFECT OF \bar{z} OF SYMMETRIC BALLAST MASSES ON α

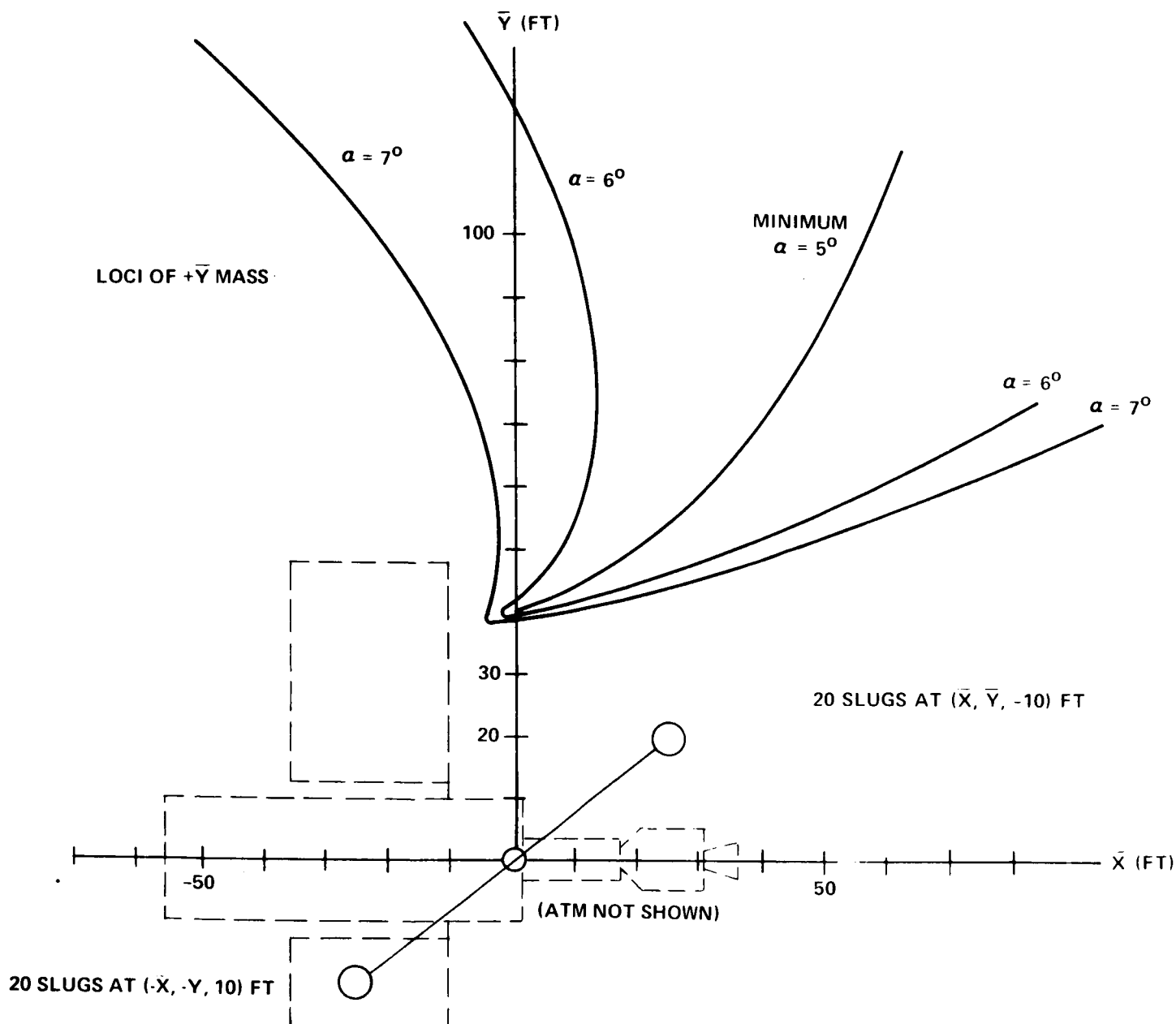


FIGURE 23 - THE EFFECT OF x, y OF SYMMETRIC BALLAST MASSES ON α

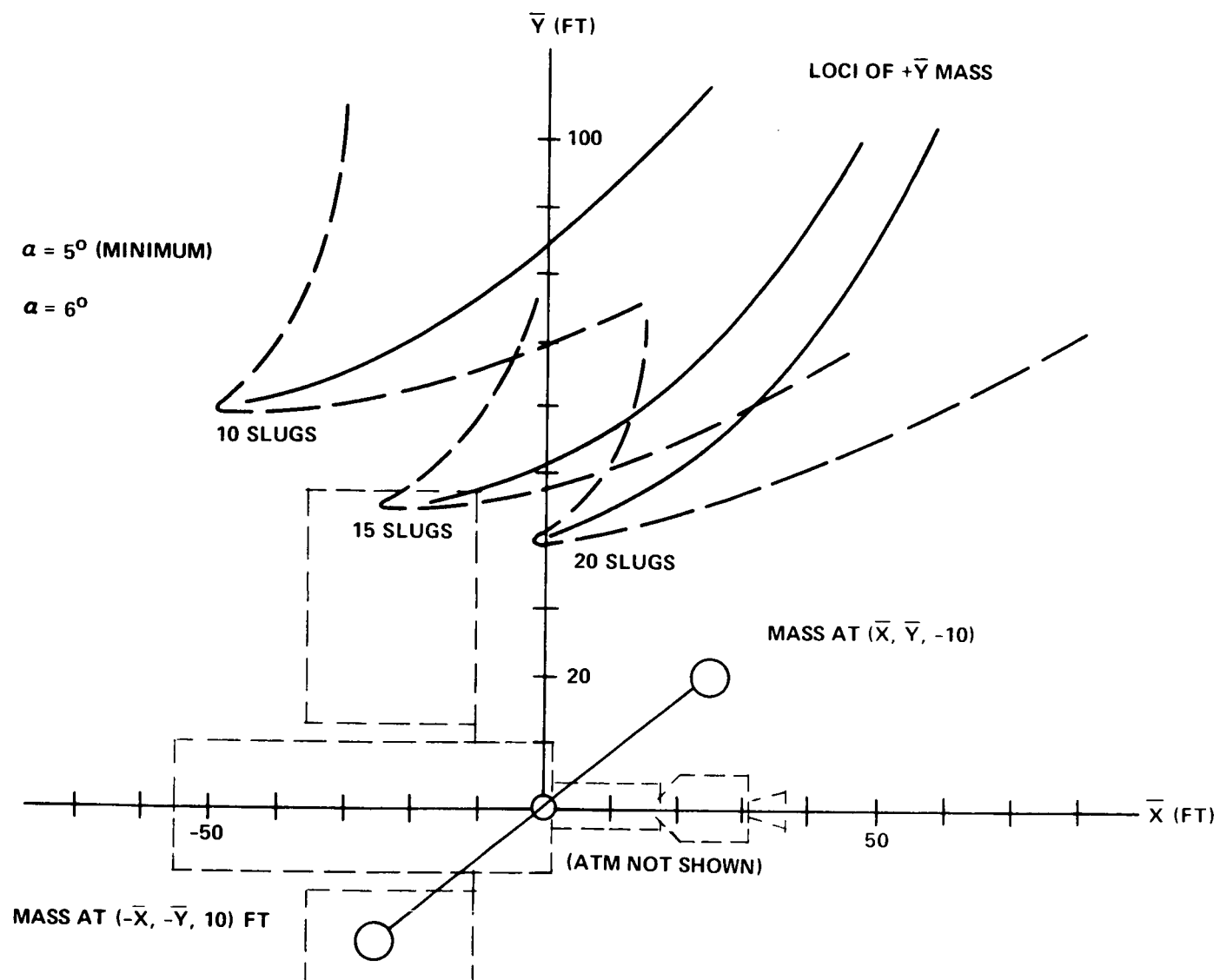


FIGURE 24 - THE EFFECT OF SIZE OF BALLAST MASS ON α

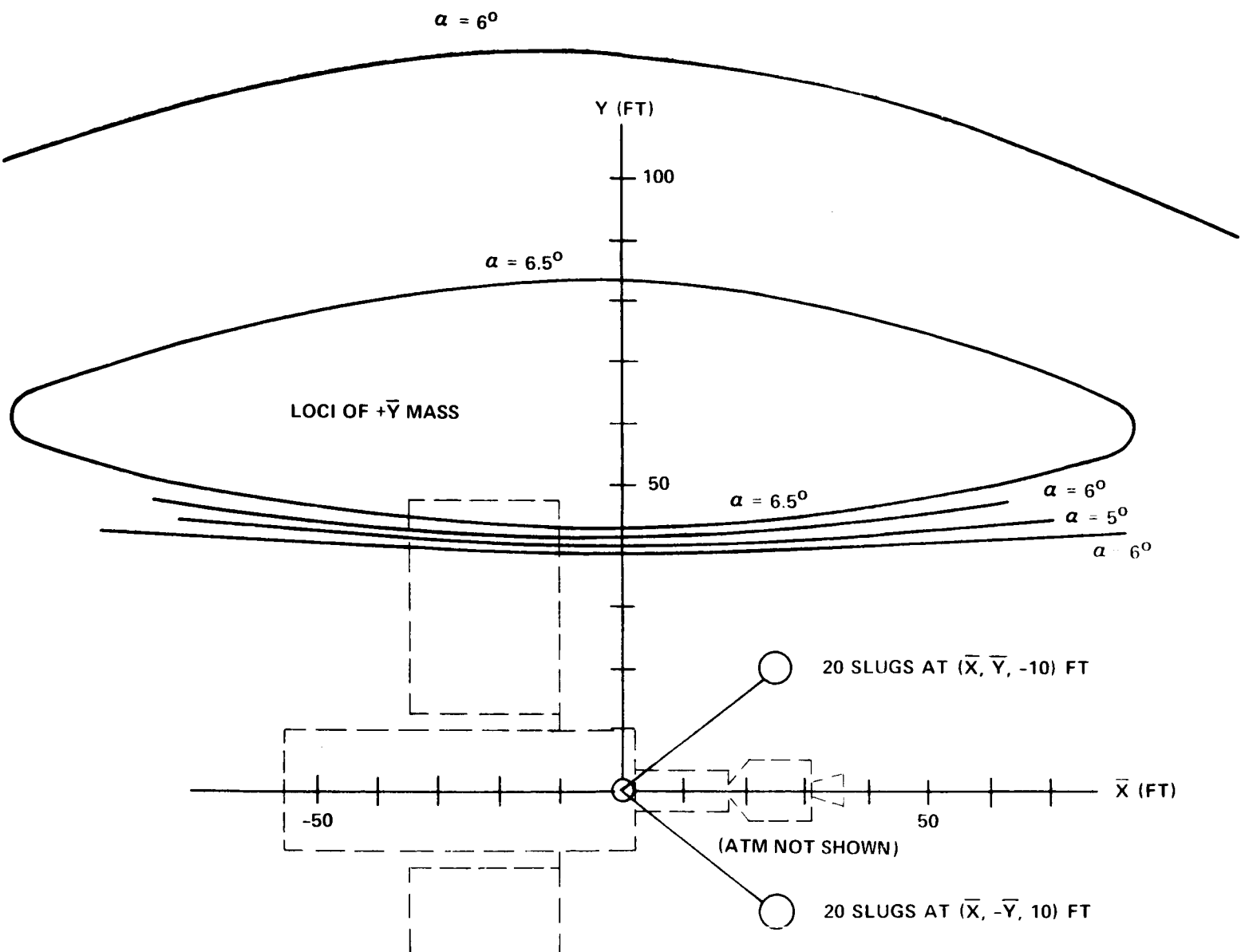


FIGURE 25 - EFFECT OF NON-SYMMETRIC BALLAST MASSES ON α